Research Article

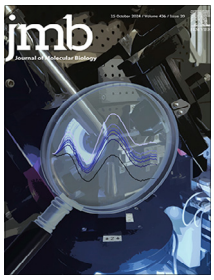

The Host miR-17-92 Cluster Negatively Regulates Mouse Mammary Tumor Virus (MMTV) Replication Primarily Via Cluster Member miR-92a

Jasmin Baby [1,†], Bushra Gull [1], Waqar Ahmad [1], Hala Abdul Baki [1], Thanumol Abdul Khader [1,4], Neena G. Panicker [1], Shaima Akhlaq [1], Tahir A. Rizvi [2,3,4] and Farah Mustafa [1,3,4,*]

*1 - **Department of Biochemistry and Molecular Biology,** College of Medicine & Health Sciences (CMHS), United Arab Emirates (UAE) University, Al Ain, UAE*

*2 - **Department of Microbiology and Immunology,** College of Medicine & Health Sciences (CMHS), United Arab Emirates (UAE) University, Al Ain, UAE*

*3 - **Zayed Center for Health Sciences (ZCHS),** UAE University, Al Ain, UAE*

*4 - **ASPIRE Research Institute in Precision Medicine,** Abu Dhabi, UAE*

Correspondence to Farah Mustafa: *Department of Biochemistry & Molecular Biology, College of Medicine and Health Sciences (CMHS), Tawam Hospital Complex, UAE University, P.O. Box 15551, Al Ain, UAE. 201790693@uaeu.ac.ae, jnull@mail.ubc.ca (J. Baby), 201790692@uaeu.ac.ae (B. Gull), waqar.ahmad@uaeu.ac.ae (W. Ahmad), 201970270@uaeu.ac.ae (H.A. Baki), 201890024@uaeu.ac.ae (T.A. Khader), 201990158@uaeu.ac.ae (N.G. Panicker), 201570084@uaeu.ac.ae (S. Akhlaq), tarizvi@uaeu.ac.ae (T.A. Rizvi), fmustafa@uaeu.ac.ae (F. Mustafa)*

https://doi.org/10.1016/j.jmb.2024.168738

Edited by Eric O. Freed

Abstract

The mouse mammary tumor virus (MMTV) is a well-known causative agent of breast cancer in mice. Previously, we have shown that MMTV dysregulates expression of the host miR-17-92 cluster in MMTV-infected mammary glands and MMTV-induced tumors. This cluster, better known as oncomiR-1, is frequently dysregulated in cancers, particularly breast cancer. In this study, our aim was to uncover a functional interaction between MMTV and the cluster. Our results reveal that MMTV expression led to dysregulation of the cluster in both mammary epithelial HC11 and HEK293T cells with the expression of miR-92a cluster member being affected the most. Conversely, overexpression of the whole or partial cluster significantly repressed MMTV expression. Notably, overexpression of cluster member miR-92a alone repressed MMTV expression to the same extent as overexpression of the complete/partial cluster. Inhibition of miR-92a led to nearly a complete restoration of MMTV expression, while deletion/substitution of the miR-92a seed sequence rescued MMTV expression. Dual luciferase assays identified MMTV genomic RNA as the potential target of miR-92a. These results show that the miR-17-92 cluster acts as part of the cell's well-known miRNA-based anti-viral response to thwart incoming MMTV infection. Thus, this study provides the first evidence highlighting the biological significance of host miRNAs in regulating MMTV replication and potentially influencing tumorigenesis.

Introduction

RNA viruses have acquired various evolutionary advantages, the most important of which is their capacity to commandeer cellular machinery and elude host immune responses. These viruses are among the most common culprits responsible for clinically significant viral infections in humans, including influenza, human immunodeficiency virus (HIV), hepatitis B and C viruses (HBV & HCV), Ebola, Zika, Nipah, and more recently, the coronaviruses (SARS, MERS, COVID-19). Retroviruses are an exceptional class of RNA viruses with the capability to *retro*-transcribe their genomic RNA into double-stranded DNA, employing reverse transcriptase, an RNA-dependent DNA polymerase.[1] The mouse mammary tumor virus (MMTV) is a *betaretrovirus* shown to cause breast cancer and lymphoma/leukemia in mice. Since its discovery in the 1930s, its antigens and sequences have been observed in human breast cancer as well, leading to the highly controversial possibility of a human mammary tumor virus (HMTV).[2–5] MMTV is a classic example of a slow-transforming retrovirus that causes breast cancer via insertional mutagenesis in mice over a period of 6–9 months where it integrates upstream of host genes involved in regulating growth and proliferation, such as *Wnt1, Fgf3, Rspo, and Notch4*.[6,7] Additionally, at least two structural genes of MMTV, *gag* and *env*, have also been reported to have oncogenic potential.[8–11] Despite extensive research into understanding MMTV replication since its discovery as a 'milk-borne agent' in 1936, there continues to be inadequacies in understanding the dynamics of viral replication, virus-host interactions, and pathogenesis, especially how MMTV interacts with the cellular RNA Interference (RNAi) machinery.

MicroRNAs (miRNAs) belong to the RNAi machinery, a class of small non-coding RNAs that are super-regulators of gene expression.[12–14] They silence gene expression by targeting the 3′ untranslated region (UTR) of mRNAs primarily in a sequence-specific manner; however, they can also target the 5′ UTR and the coding regions of an mRNA.[15] Encoded within the genome, the biogenesis of miRNAs begins in the nucleus and closely follows the typical transcription activation and splicing steps of any protein-coding mRNA, except that miRNAs additionally use a unique set of enzymes and proteins (Drosha, DCGR8, Dicer, etc.) for their processing; i.e., undergoing multiple cleavages in a stepwise manner to form the mature miRNA from the primary RNA.[16,17] Thus, processing of the primary miRNA by these enzymes starts from the nucleus to the cytoplasm, giving rise to the final dsRNA effector molecule, the mature miRNA, that comprises of a guide and a passenger strand. The guide strand forms a complex with the RNA-induced silencing complex (RISC), and identifies target mRNAs based on complementarity, which are then routed to cytoplasmic processing bodies (p-bodies) and marked for degradation. The two strands of the mature miRNA have distinct "seed" sequences and either of these have the potential to be loaded onto RISC to serve as the guide strand. This is an aspect critical in mRNA targeting and gene regulation, an area only now being unraveled.[18]

Functioning as a part of the natural cellular RNAi machinery, miRNAs not only regulate changes in gene expression during development, but also serve as an "anti-viral" defense mechanism against invading viruses, a process that has been observed in a variety of taxa, including plants, nematodes, and arthropods.[19–22] The "anti-viral" miRNAs are induced in the presence of exogenous RNA in the host, which are identified by miRNA-viral RNA sequence complementarity in which the viral RNA is subjected to degradation by cellular enzymes.[23,24] While the anti-viral potential of the RNAi machinery is well known since the 1990s, it was first clearly demonstrated in *C. elegans* when inhibition of the vesicular stomatitis virus (VSV) was observed in mutant worms with an enhanced small RNA interference potential.[25] Viruses, on the other hand, can manipulate host miRNAs to prevent the cell's anti-viral response or favor virus propagation.[26–29] For example, HCV can significantly enhance levels of miR-373 in hepatocytes, which leads to attenuation of the JAK/STAT pathway via JAK1 and IRF9 at the RNA level, thereby counteracting interferon-mediated anti-viral responses in the cell.[30] Similarly, the human respiratory syncytial virus (RSV)-encoded proteins NS1 and NS2 can up-regulate cellular miR-29a to regulate the suppression of the interferon receptor, thus aiding viral replication stimulated by NS1.[31]

While miRNAs normally are expressed from single genes, nearly 50% of miRNAs in *Drosophila melanogaster* and more than one-third of human miRNA genes are clustered together and expressed in polycistronic miRNA clusters, where a single parent transcript produces multiple mature miRNAs.[32–35] miR-17-92 is the first oncogenic miRNA cluster (oncomiR-1) to be described and studied extensively for its role in cell cycle regulation, differentiation, apoptosis, and tumorigenesis.[32,36–41] Amplified in hematopoietic malignancies and solid tumors, a study of B-cell lymphomas in an Eμ-*myc* transgenic mice was the first to point out the cluster and its oncogenic potential.[42,43] The miR-17-92 host gene (MIR17HG) is located in the non-transcribed region of human chromosome 13 (13q31.3) and chromosome 14 in mice (14E4), devoid of protein coding potential. The cluster is a polycistron, coding for a single RNA transcript that is processed into six mature miRNAs: miR-17, miR-18a, miR-19a, miR-20a, miR-19b-1, and miR-92a-1.[42] These mature miRNAs are conserved throughout vertebrates and paralogues of the cluster exist, namely miR-106a-363

(Xq26.2) and miR-106b-25 (7q22.1), arising due to gene duplication events.[44,45] As mentioned earlier, miRNAs identify their target genes and exert post-transcriptional modulation via their seed sequences; i.e., nucleotides 2–8 of the mature form, to engage in the mRNA recognition/targeting event.[46] Based on their seed sequences, the miR-17-92 gene cluster and its homologs are categorized into four families: the miR-17 family (miR-17, miR-20a/miR-20b, miR-106a/miR-106b, and miR-93), the miR-18 family (miR-18a/miR-18b), the miR-19 family (miR-19a/miR-19b), and the miR-25 family (miR-25, miR-92a, and miR-363).[47]

With extensive research on the miR-17-92 cluster and its relevance as oncomiR-1 in tumor development and progression, in comparison, not much has been explored on the functional importance of this miRNA cluster in thwarting or facilitating viral infections. The miR-17-92 cluster exhibits both anti- and pro-viral roles, making it a key target in the development of anti-virals and miRNA-based therapeutics.[48] For example, in HBV infection, the cluster's activation inhibits virus replication,[49] while in enterovirus-71 (EV-71) infection, the virus disrupts the cluster's anti-viral effect via promoter methylation, enhancing replication.[50] Conversely, in Kaposi's sarcoma-associated herpesvirus (KSHV) infection, the activated cluster promotes tumor growth by down-regulating the TGF pathway.[51] Triboulet et al. first identified the cluster's anti-viral potential against retroviruses, where it suppresses HIV replication by targeting histone acetylase PCAF, a key factor in HIV-1 activation by its Tat protein.[52] Bioinformatics predicted four target sites for miR-17 and miR20a on PCAF's 3′ UTR, and therapeutic strategies using multiplex miRNA technology with engineered conserved anti-HIV sequences in the miR-17-92 polycistron have shown promise in combating HIV-1.[53]

Viral genomes can also encode miRNAs that can help facilitate virus replication and manipulate anti-viral host immune responses, especially in DNA viruses.[54–57] However, we have recently shown that the MMTV genome does not encode miRNAs; rather it dysregulates expression of host miRNAs, especially the miR-17-92 cluster.[58] Based on these observations, the current study was undertaken to find any functional interaction between MMTV and the miR-17-92 cluster at the cellular level and its consequences for virus replication. Since an up-regulation of several cluster members was observed in not only mouse mammary tumors that express one of the highest levels of the virus, but also infected lactating mammary glands,[58] we hypothesized that the cluster was facilitating MMTV replication in mammary epithelial cells. However, it was also possible that early in infection, the cluster keeps the viral replication in check as an anti-viral response for which miRNAs are more well-known for, and later on, the virus somehow overcomes this suppression. Interestingly, we observed the latter and found an anti-viral association between miR-17-92 and MMTV with the cluster leading to repression of MMTV expression, despite its high level of expression in mammary glands and mammary tumors. Furthermore, we identify miR-92a as one of the critical anti-viral components of the cluster that inhibits MMTV gene expression and replication by targeting its genomic RNA.

Results

The miR-17-92 cluster members are dysregulated upon MMTV expression

To explore whether MMTV could interfere with the expression of the miR-17-92 cluster, we interrogated our miRNAseq data of a mouse mammary epithelial cell line HC11 compared to the same cell line expressing MMTV, HC11-MMTV.[59,60] Mammary epithelial cells are the most permissive cells for MMTV infection *in vivo,* responsible for ensuring the passage of the virus from the mother to the pups via breast milk; additionally, these are the main cells targeted for mammary tumorigenesis in mice.[6,7] Figure 1A reveals the heat map of the expression of the cluster members in the two cell lines (two biological replicates, 1 & 2, are shown for each). As can be seen, a distinct dysregulation of the cluster member expression could be observed upon MMTV expression. Fold-change analysis of differential gene expression between the two cell lines revealed that while the expression of some of the cluster members was not much affected (miR-17-3p and miR19a-3p), a distinct up-regulation could be observed in the expression of other cluster members, such as miR-18a and miR-92a, with miR-92a showing the highest induction at 4-folds upon MMTV expression (Figure 1B). It is to be kept in mind that miRNA gene expression profiling studies have revealed that even subtle changes of 1.5- to 2-fold can have significant impact on target gene expression in cells, depending upon factors such as the target miRNA under study, whether it is a cluster or monomeric miRNA, the level of target gene expression, the number of mRNA binding sites, etc.[61–63] Other cluster members not shown in Figure 1B, did not demonstrate any substantial levels of expression in the HC11 cells.

Being of mouse and mammary epithelial origin, HC11 are the most appropriate cells to study MMTV replication in its relevant context; however, they express endogenous strains of MMTVs that are found ubiquitously in most mouse species.[6,7] These endogenous strains of MMTV (specifically *mtv-6, mtv-8,* and *mtv-9* in HC11 since they are of BALB/c origin) are defective for replication, but are able to express parts of their genomes that could have confounded our results.[64,65] Therefore, to study the interaction between MMTV and the miR-17-92 cluster further, we decided to use the human embryonic kidney cell line HEK293T. Since this cell

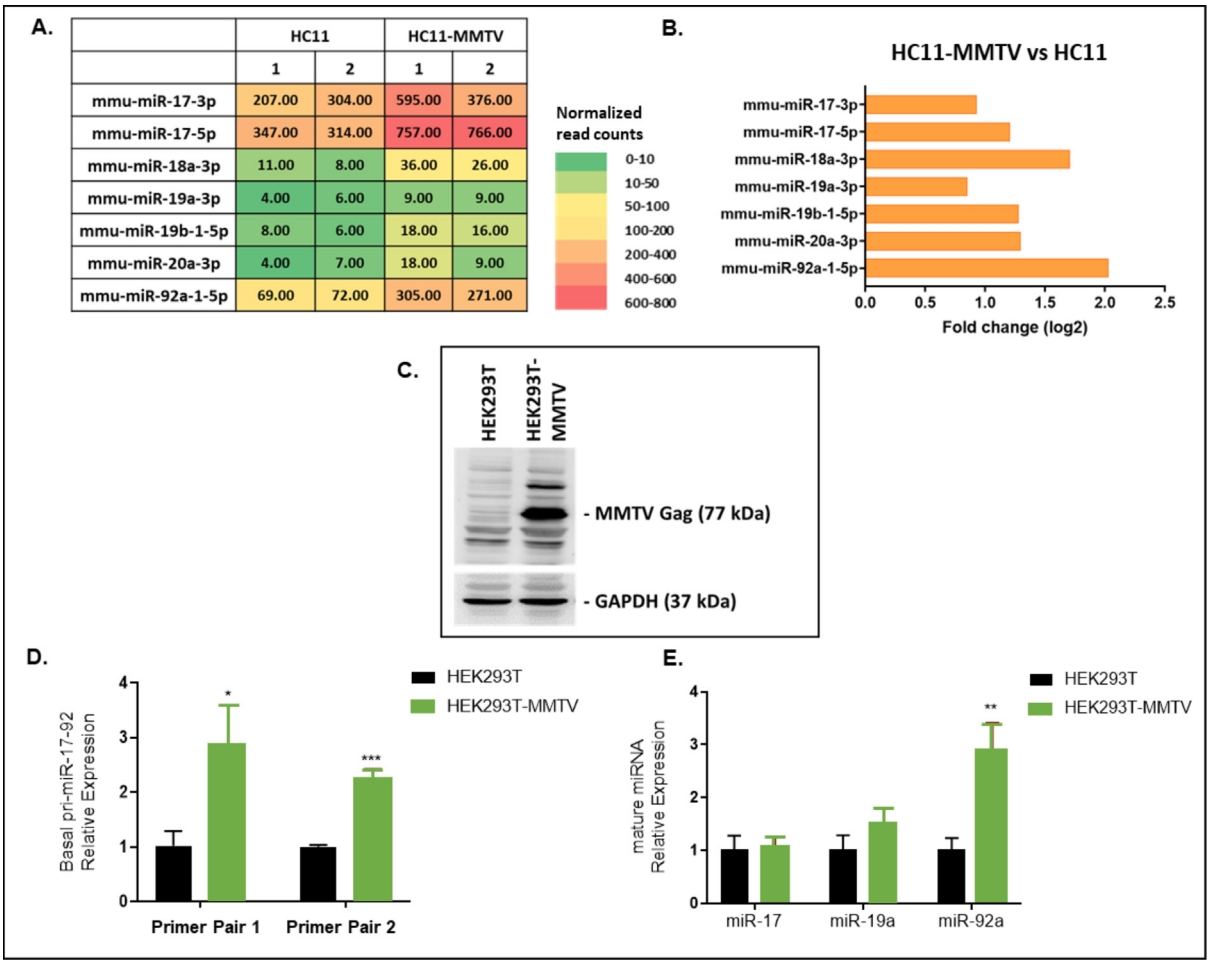

Figure 1. The miR-17-92 cluster members are dysregulated upon MMTV expression. (A) Heat-map of miR-17-92 cluster upon small miRNAseq analysis of the normal mouse mammary epithelial cell lines, HC11 and HC11-MMTV. The miRNAseq was conducted on two biological replicates shown as 1 and 2. The numbers in the table represent the normalized reads observed upon miRNAseq. **(B)** Fold-change analysis of mature miR-17-92 cluster member expression using the miRNAseq data from HC11 cells. The Q-value (equivalent of *p*-value corrected for multiple test hypothesis) for each of the miRNA shown was statistically significant ($Q < 0.005$). **(C)** Western blot analysis of HEK293 and HEK293T cells expressing MMTV using an anti-MMTV Gag antibody. An antibody against a housekeeping gene (GAPDH) was used as a loading control. **(D)** Quantitative RT-PCRs (RT-qPCRs) to assess endogenous levels of the primary form of miR-17-92 cluster upon MMTV expression in HEK293T cells. β-Actin was used as the endogenous control. **(E)** RT-qPCR analysis of mature miR-17, miR-19a and miR-92a in HEK293T cells. U6 was used as the endogenous control. All experiments were carried out in triplicates. Statistical significance is shown as * where $*p \leq 0.05$; $**p \leq 0.01$, and $***p \leq 0.001$.

line is of human origin, it is devoid of any endogenous strains of MMTV, yet it can express MMTV efficiently and produce infectious pseudotyped virus particles upon transfection.[66–69]

Towards this end, similar to HC11, the HEK293T cells were transfected with HYBMTV, a replication-competent molecular clone of MMTV,[70] to establish an HEK293T-MMTV stable cell line constitutively expressing the virus (Figure 1C). Quantitative real-time PCR with two primer sets, primer pair 1 (OFM 446/447) and primer pair 2 (OFM450/451), that targeted the primary (pri)-form of the cluster, revealed that MMTV significantly enhanced expression of the primary form of the miR-17-92 cluster by more than 2.5-fold relative to HEK293T cells alone (Figure 1D). Subsequently, the levels of some of the mature cluster members (miR-17, miR-19a and miR-92a) were assessed using TaqMan miRNA assays to determine if the level of mature miRNAs followed the same course. Similar to the HC11 cells, a significant 2.9-fold increase in the endogenous levels of miR-92a was observed, while levels of miR-17 and miR-19a were not affected significantly (Figure 1E). These data reveal that MMTV enhanced expression of the primary form of the miR-17-92 cluster, while its effect on individual mature cluster members varied with miR-92 being affected the most. They also confirm that observa-

tions made in the HEK293T cells recapitulated what was observed in the more relevant HC11 cells, making our HEK293T system valid for further investigation of the interactions between MMTV and the miR-17-92 cluster members.

MMTV expression is significantly down-regulated upon miR-17-92 over-expression

Previously, it has been shown that host miRNAs can have anti-viral potential where activation of these miRNAs leads to reduction in virus expression.[50,49,71,52] Since miR-92a was observed to be the most affected cluster member upon MMTV expression in both cell lines, we asked whether miR-92a could have a negative feedback relationship with viral replication as an anti-viral miRNA. To test this hypothesis, expression plasmids carrying either the full cluster, a truncated version of the cluster expressing miR-19a-20a-19b (miR-19/20) but lacking miR-92a, or miR-92a only were transfected into HEK293T-MMTV cells to create miRNA over-expression (OE) stable cell lines along with a control expressing the empty vector (EV) without any miRNA insert (Figure 2A and B). The miRNA over-expression phenotype was confirmed using TaqMan miRNA assays and its effect on MMTV expression was assessed at the RNA and protein levels.

As can be seen, the miR-17-92 full cluster OE cells showed a significant increase in the amounts of pri-miR-17-92 produced (5–7 folds) compared to the EV-expressing cells (Figure 2C). Next, we analyzed the expression of some of the individual members of the cluster in this cell line. A statistically significant over-expression of cluster members miR-17 and miR-19a could be observed in the 1.3- to 7.7-fold range; however, miR-92a was upregulated the most (~225-folds) (Figure 2D). The miR-19/20 cell line expressing the partial cluster (miR-19a-20a-19b), showed an unexpected down-regulation in the levels of miR-19a (Figure 2E), while the miR-92a over-expression cell line confirmed a clear and significant 7-fold over-expression of miR-92a (Figure 2F). Next, the functional consequence of miR-17-92 cluster over-expression on MMTV expression was assessed at the protein and RNA levels. Test of the MMTV Gag structural gene expression levels were observed to be down-regulated at the protein level when compared to the empty vector control in all the three OE cell lines (Figure 2G). Densitometric analysis on the same revealed that the level of repression of MMTV expression by miR-92a alone was comparable to that of its expression from the full cluster (Figure 2G). This down-regulation of MMTV expression was confirmed at the RNA level where over-expression of either the full miR-17-92 cluster, the miR-19/20 partial cluster, or miR-92a only significantly down-regulated MMTV mRNA expression (Figure 2H). Subsequently, the effect of the full cluster and miR-92 over-expression on MMTV virus particle production and genomic RNA packaging was assessed using RT-qPCR. As can be seen, the amount of genomic RNA expressed in the cells was significantly down-regulated in both the miR-17-92 full cluster and miR-92a over-expressing cells (Figure 2I). This decrease was reflected in reduced amounts of gRNA packaged into the virus particles with the miR-92a over-expressing cells showing the most inhibition (Figure 2I). This observation was confirmed by western blot analysis of virus particles produced in each cell line. As can be seen, the level of virions produced in the miR-17-92 cluster and miR-92a over-expressing cells was drastically reduced compared to the control EV-expressing cells (Figure 2J). Considering that the unspliced, full-length genomic RNA in retroviruses is used not only to produce the structural polyprotein such as Gag, but also for its encapsidation into the newly-assembling virus particles, this result suggests that expression of the miR-17-92 cluster, and in particular its miR-92a component, results in down-regulation of virus replication, perhaps as an anti-viral response of the cells to MMTV infection.

Anti-miRNA oligo-based inhibition of miR-17-92 and miR-92a rescues MMTV expression

To validate these findings, we took the reverse approach where modified anti-miRNA oligos were used to inhibit mature forms of cluster members in the three different OE cell lines. Results from these analyses were compared to treatment of the same cell lines in parallel with control scrambled oligos specific for each miRNA inhibited (NC). To inhibit miRNA abundance in the miR-17-92 HEK293T-MMTV OE cell line, we took the approach of using a combination of anti-miR-17, -19a and -92a inhibitors at a concentration of 15 pmol each. Similarly, 15 pmol of anti-miR-19a and 15 pmol of anti-miR-92a were used individually to suppress miRNA overexpression in the miR-19/20 and miR-92a OE cell lines, respectively. TaqMan miRNA assays were carried out to quantify and confirm the inhibition of miR-17, miR-19a and miR-92a. Interestingly, in the miR-17-92 OE cell line treated with the anti-miRNA cocktail, no significant reduction in the targeted miRNAs was observed (Figure 3A), while, the miR-19/20 OE cell line treated with anti-miR 19a showed a downward trend of miR-19a suppression that was statistically significant (Figure 3B). The most significant inhibition, however, was observed in the miR-92a OE cell line treated with anti-miR-92a where ~80% decrease in miR-92a population was detected (Figure 3C). Despite variable levels of respective miRNA inhibition obtained, we could discern some rescue of MMTV Gag (Pr77) expression in all the cell lines treated with the respective anti-miR oligo

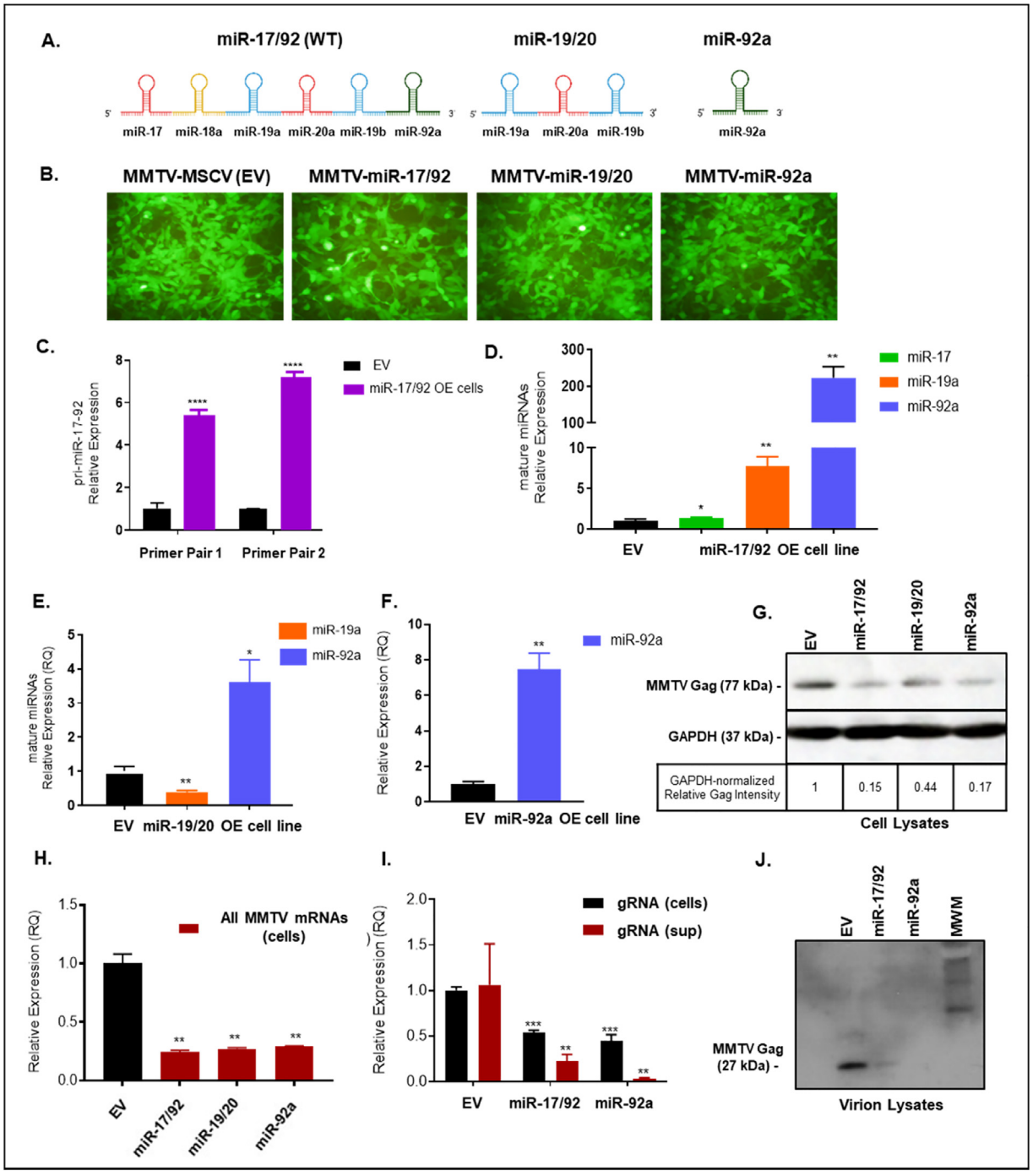

Figure 2. Over-expression of the miR-17-92 cluster down-regulates MMTV expression. (A) An illustration of the miR-17-92 cluster, its truncated form miR-19a-20a-19b, and miR-92a over-expressed (OE) exogenously in the HEK293T-MMTV cells. **(B)** GFP-positive stably-transfected cells selected in puromycin and visualized using a fluorescent microscope (10x). **(C)** Expression of pri-miR-17-92 in miR-17-92 OE cell line quantified using a SYBR Green qPCR assay. **(D)** TaqMan miRNA assays used to quantify expression of mature miR-17, miR-19a, miR-92a in the miR17-92 OE cell line, **(E)** miR-19/20 OE cell line, and **(F)** miR-92a OE cell line. U6 snRNA was used as the endogenous control in these assays. **(G)** Western blot analysis of MMTV Gag expression in cell lysates. **(H)** MMTV RNA-specific TaqMan assay to quantify all MMTV messages in the three OE cell lines. **(I)** MMTV genomic RNA was assessed using gRNA-specific MMTV TaqMan assay in the miR-17-92 cluster OE and the miR-92a OE cells and virus particles isolated from culture supernatants (sup) via ultracentrifugation. The empty vector (EV) was designated as 1 in all analyses. Mean ± SD (n = 3). Statistical significance is shown as * where $*p \leq 0.05$; $**p \leq 0.01$, $***p \leq 0.001$, $****p \leq 0.0001$. **(J)** Western blot analysis of viral particles harvested from culture supernatants in the respective miRNA OE stable cell lines.

inhibitors compared to the scramble negative control (NC1-3) at the protein level (Figure 3D).

To quantitate the effect of the anti-miR oligo inhibitors on virus expression, total RNA from the three cell lines was subjected to MMTV-specific genomic RNA RT-qPCR. As can see seen, a significant up-regulation in MMTV gRNA expression was observed in the miR-17-92 OE cell line treated with anti-miR-17 + anti-miR-19a + anti-miR-92a inhibitor cocktail compared to the negative scramble control treatment (Figure 3E). However, no significant rescue of MMTV gRNA expression could be observed with treatment of the miR-19/20 OE cells with the anti-miR-19 oligo (Figure 3F). In contrast, some rescue could be observed of MMTV gRNA expression with the anti-miR-92a inhibitor in the miR-92a OE cell line, though it was not statistically significant (Figure 3G). To determine whether the effect of anti-miR-92a was real, the experiment was repeated in the miR-92a OE cell line with increasing doses of the anti-miR-92a inhibitor oligo. Treatment of the miR-92a OE cell line with increasing concentrations of the scrambled oligo (NC) did not affect MMTV expression which was repressed due to the over expression of miR-92a in this cell line (Figure 3H). However, a significant rescue of MMTV Gag protein expression could be observed upon increasing amounts of the anti-miR-92a inhibitor oligo that could be visualized on a western blot (Figure 3H). Although not dose-dependent since probably maximum suppression had already been achieved at the lowest dose of 15 pmol, these observations are consistent with the result that the miR-17-92 cluster suppresses MMTV gene expression via miR-92a. The severe repression of MMTV in the control (NC) lanes of miR-92a OE cell line in Figure 3H treated with the scrambled oligo instead of anti-miR-92a oligo reconfirms this conclusion.

Plasmid-based miRNA inhibition (PMIS) of miR-17-92 cluster members up-regulates MMTV expression

To investigate these findings further, a plasmid-based approach to miRNA inhibition was used in which vectors expressing anti-sense miRNAs were used that repress miRNA functionality by forming a stable PMIS-miRNA complex.[72] Towards this end, three stable PMIS cell lines were established in HEK293T-MMTV cells against miR-17 (PMIS 17), miR-92a (PMIS 92) and empty control vector (EV) that constitutively expressed the anti-sense miRNA or the empty vector as a control. These cell lines were tested for the expression of the respective miRNAs inhibited using specific TaqMan miRNA assays (Figure 4. Interestingly, these assays revealed that the PMIS vectors could not down-regulate the targeted endogenous miRNA population; i.e., while a slight downward trend could be observed of miR-17 that was not statistically significant, an up-regulation of ~1.5-folds was observed for miR-92a which was statistically significant (Figure 4A & 4B). This was surprising and we wanted to test whether this observation was real or an artefact of the PMIS vector system. We hypothesized that the miRNA-anti-sense PMIS complex probably forms a duplex that is stable and was being detected in these assays. Therefore, despite a physical lack of inhibition of the test miRNAs, miR-17 and miR-92a, we tested for a functional loss of the tested miRNAs. This was achieved by analyzing the expression of the validated target of miR-17, the phosphatase and tensin homolog (PTEN) mRNA. As can be seen, a 2-fold up-regulation of PTEN transcript was observed in the PMIS 17 cell line that was statistically significant, confirming the functional inhibition of miR-17 in the PMIS stable cell line (Figure 4C). Based on these results, we analyzed MMTV expression in PMIS 17 and PMIS 92 stable cell lines. As expected, despite a lack of physical down-regulation of the targeted miRNAs, we observed an up-regulation of the MMTV Gag protein and genomic RNA in a statistically significant manner (Figure 4D and E). These results confirm the suppressive role of not only miR-92a, but also miR-17 in MMTV gene expression.

miR-92a is a critical anti-viral component of the miR-17-92 cluster

Next, we used a mutational approach to further study the role of miR-92a as an anti-viral cellular component against MMTV since its levels were the most affected in MMTV-expressing HC11 and HEK293T cells (Figure 1), and also because it does not share seed sequences with any other member of the cluster[73,74] that could have confounded our results. Plasmid vectors carrying the wild-type miR-17-92 (WT) cluster, miR-17-19b (Δ92a)- a miR-92a-deleted version of the whole cluster, and a substitution mutant of the miR-92a seed sequence in the cluster, miR-17-92aMUT (92aMUT), were transiently transfected into HEK293T-MMTV cell line to determine whether they could affect MMTV expression.

As expected, expression of the WT miR-17-92 cluster down-regulated MMTV expression at the protein level compared to the empty vector control (EV) (Figure 5A). This phenotype was reversed when the miR-92 seed sequence was either deleted from the cluster or mutated via a substitution (Figure 5B). Quantitation of MMTV expression by the TaqMan RT-qPCR assay confirmed these results where expression of the wild type cluster resulted in down-regulation of MMTV genomic RNA expression in a statistically-significant manner, while either deletion or mutation of the miR-92a component of the cluster rescued the levels to wild type levels (Figure 5C). These results suggest that miR-92a is the major anti-viral component of the miR-17-92 cluster in controlling MMTV replication in the cell.

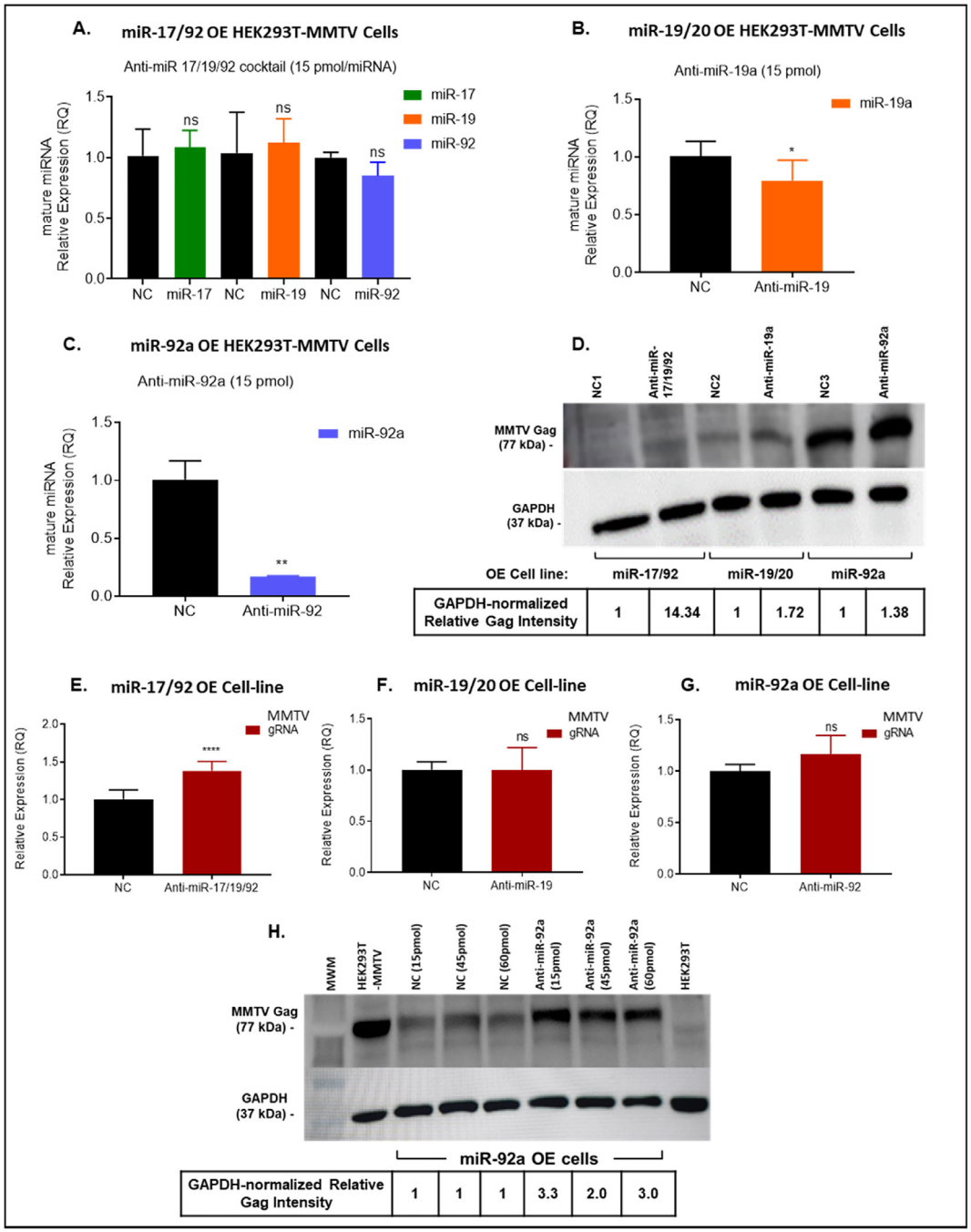

Figure 3. Mir-17-92 cluster and miR-92a inhibition rescues MMTV genomic RNA expression. TaqMan miRNA assays were used to quantify: **(A)** miR-17, miR-19a and miR-92a in miR-17-92 over expression (OE) cell line, **(B)** miR-19a in the miR-19a-20a-19b OE cell line, and **(C)** miR-92a in the miR-92a OE cell line. U6 snRNA was used as the endogenous control in the miRNA RT-qPCR assays. The error bars represent ± SD. NC, negative control scrambled oligo specific for each miRNA inhibitor used. **(D)** Western blot analysis of whole cell lysates (40 μg) from the miRNA OE cell lines treated with miRNA inhibitors for MMTV Gag expression. GAPDH was used as the internal control. Expression of the MMTV genomic RNA was quantified in the: **(E)** miR-17-92 OE cells treated with a cocktail of anti-miR-17, -19, & -92a oligos, **(F)** miR-19a-20a-19b OE cells treated with anti-miR-19a oligos, and **(G)** miR-92a OE cells treated with anti-miR-92a oligos. β-Actin was used as the internal control in the MMTV TaqMan RT-qPCR assays. The empty vector (EV) was designated as 1 in all analyses. Mean ± SD ($n = 3$). **(H)** Western Blot analysis of whole cell lysates (50 μg) from the miR-92a OE cell line treated with anti-miR-92a oligos at varying concentrations. GAPDH was used as the internal control. Statistical significance is shown as * where *$p \leq 0.05$; **$p \leq 0.01$, ***$p \leq 0.001$, ****$p \leq 0.0001$. ns, not significant; ns ($P > 0.05$).

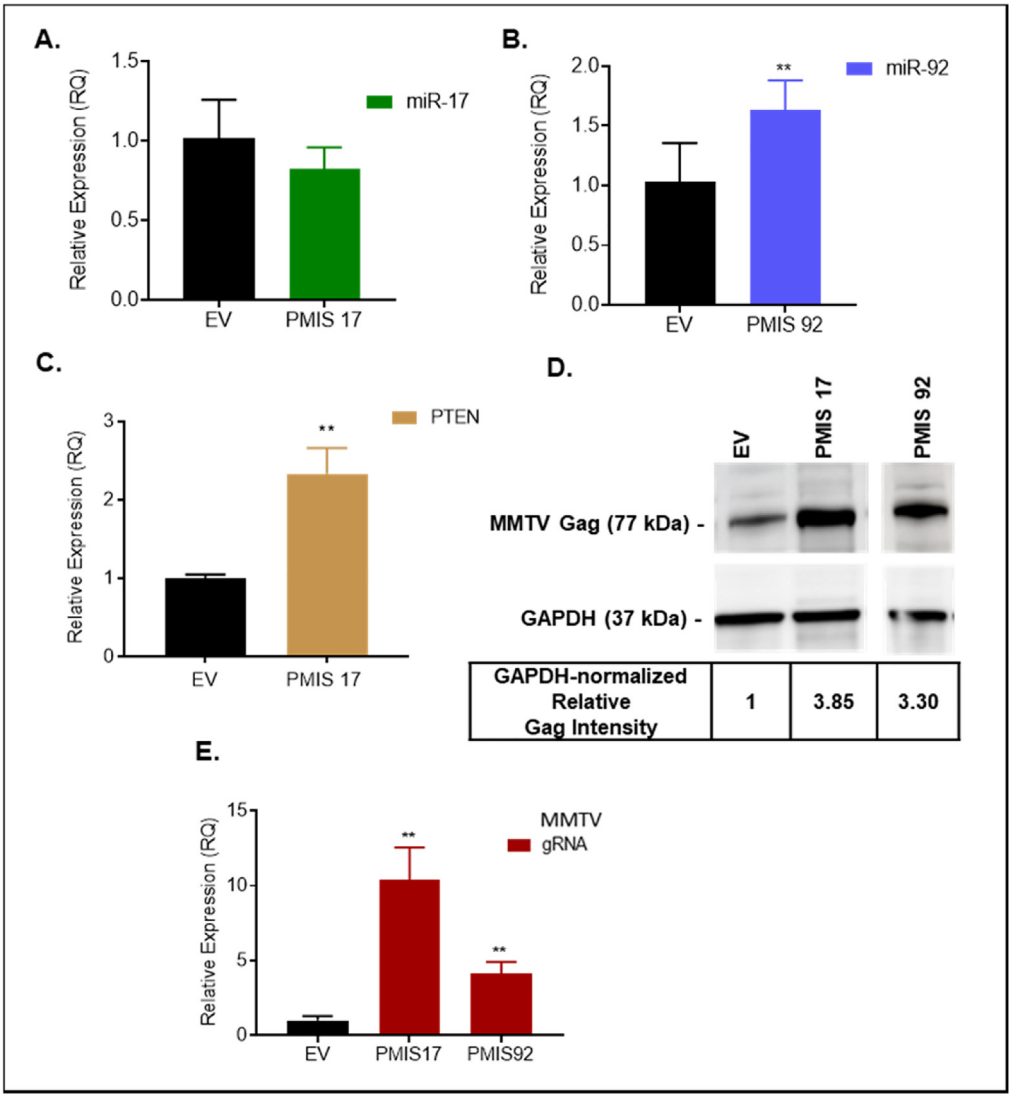

Figure 4. Rescue of MMTV expression upon plasmid-based miRNA inhibition. **(A)** Mature miR-17 and **(B)** miR-92a levels were quantified in their respective PMIS inhibitor expressing cell lines using TaqMan miRNA RT-qPCRs. U6 snRNA was used as the endogenous control. **(C)** Expression of miR-17 target, PTEN was quantified using RT-qPCR; β-Actin was used as the internal control. **(D)** Western blot analysis of MMTV Gag expression across the three cell lines using 50 μg protein. GAPDH served as the endogenous control. **(E)** The expression of all MMTV transcripts were quantified using TaqMan RT-qPCRs with β-Actin as the internal control. The empty vector (EV; the PMIS backbone without any insert) was designated as unit 1 in all experiments with means represented as ±SD (n = 3). Statistical significance is shown as * * where *$p \leq 0.05$ and **$p \leq 0.01$.

The miR-17-92 cluster interacts with the MMTV genome

Following the demonstration of a repressive role of miR-92a in MMTV expression, we aimed at identifying its probable target sites on the MMTV genome using Sfold STarMir, a crosslinking immunoprecipitation (CLIP)-based prediction software with combined algorithms of RNAhybrid and logistic thermodynamic probability.[75,76] Bioinformatic analysis of the data revealed thousands of putative binding sites of the miR-17-92 cluster members on the viral genome. The application of stringent parameters (ΔGhybrid: ≥ -20 kcal/mol; Logistic probability score above 0.7) reduced these to a total of 74 high probability binding sites that were spread across the MMTV genome and targeted all the known mRNAs of the virus, including the genomic RNA that also serves as the mRNA for the structural genes Gag/Pro/Pol (Figure 6A). These predicted miR-17-92 cluster binding sites belonged to specific members of the miRNA cluster, including miR-17, miR-18a, miR-19b, miR-20a, and miR-92a, but excluded miR-19a (Figure 6B). Interestingly, roughly two-thirds (62% or n = 46) of all predicted binding sites belonged to miR-92a, while

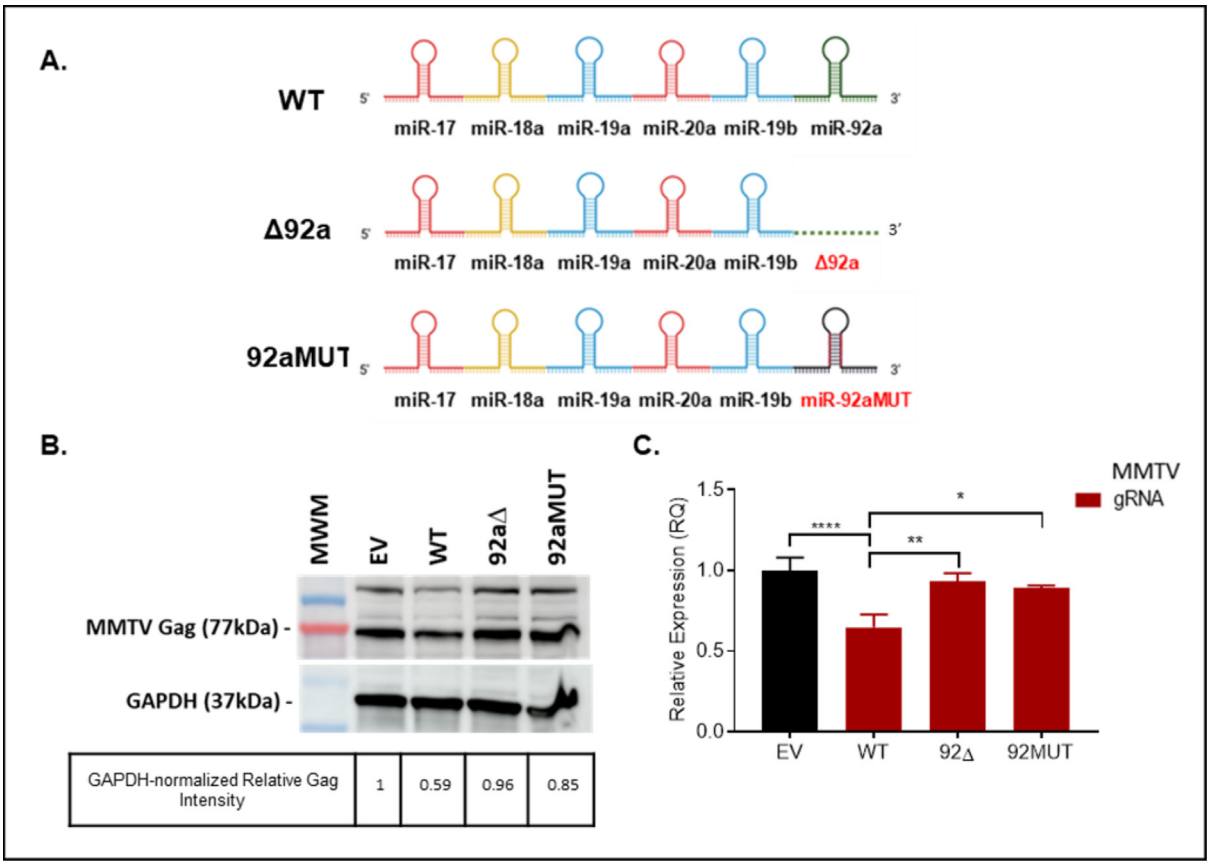

Figure 5. MMTV expression rescued upon deletion or mutation of miR-92a seed sequence. **(A)** Schematic representation of the full miR-17-92 cluster (WT), or cluster with deletion of miR-92a (Δ92a) indicated as a dashed line, or a substitution mutation of miR-92a (92aMUT) within the cluster, both highlighted in red text. **(B)** Expression of MMTV Gag quantified by western blot analysis using 40 μg lysate from the different transiently transfected cell lines; GAPDH was used as the internal control. **(C)** Quantification of all MMTV mRNAs by RT-qPCR. β-Actin used as the internal control. The empty vector (EV) was designated as unit 1 with means represented as ± SD (n = 3). Statistical significance is shown as * where $*p \leq 0.05$; $**p \leq 0.01$, $***p \leq 0.001$, and $****p \leq 0.0001$.

other members such as miR-17 and miR-19b had the least sites (Figure 6B). The 46 miR-92a binding sites were observed to be spread throughout the MMTV genome and targeted different mRNAs of the virus. Of these 46 miR-92a binding sites, ten sites were observed within the Gag region of the MMTV genome; however, one particular binding site had the highest logistic and thermodynamic probability of being a functional binding site with an 8-mer nucleotide seed type (Figure 6C), suggesting that the Gag region was a particular target of miR-92a. However, this region is found exclusively within the full-length genomic RNA and is spliced out from all the other spliced mRNAs (the blue boxed region in Figure 6A). Thus, this suggested that rather than a particular mRNA of the virus being the target of these miRNAs, it was the genomic RNA that was being targeted by the cluster members. Figure 6B highlights all the miRNAs that targeted the Gag/Pro/Pol regions. As can be seen, 40 of the total 74 miRNA binding sites (54%) were present within the Gag/Pro/Pol region of which only Gag had 16 specific binding sites, 10 of which belonged to miR-92a, including the functional binding site shown in Figure 6C.

To test the validity of these predictions and explore the possibility of a direct interaction between miR-92a and the MMTV genome, the Gag region of the MMTV genome present exclusively in the full-length genomic RNA and containing the predicted functional binding site, in addition to the 15 others, was cloned into the miRNA target plasmid, pmirGLO (Promega), creating GagGLO (Figure 7A). The Gag region was inserted in between the *firefly luciferase* gene and the SV40 poly A sequences, thus creating a fused Luciferase-Gag transcript containing the putative miR-92a target sites. The pmirGLO vector contains a second luciferase gene, *renilla luciferase*, expressed from an independent promoter that was used to internally normalize the transfection efficiencies. The GagGLO plasmid was tested in parallel with the control pmirGLO vector in the HEK293T and HEK293T-MMTV cells

A.

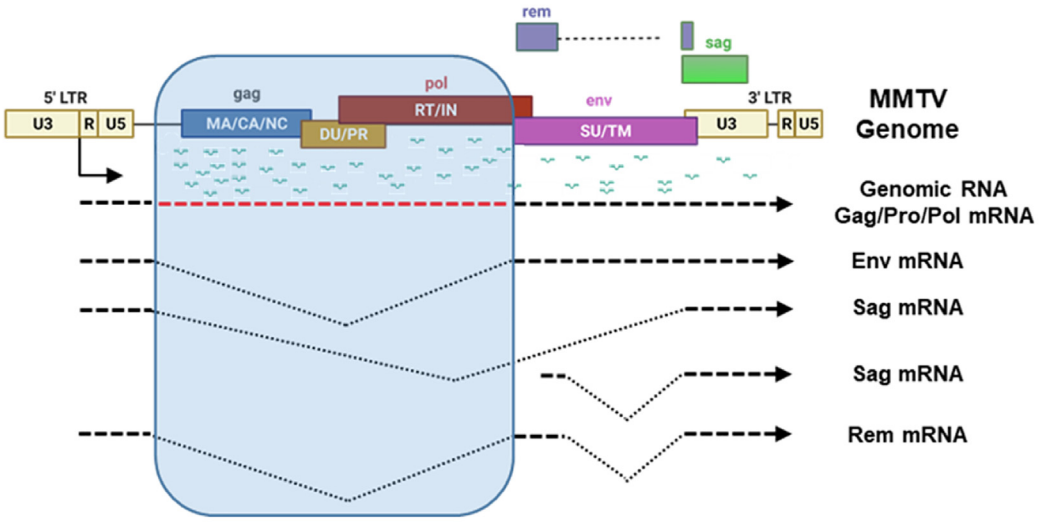

B.

miRNA	No. of sites	Target RNA Target Region* (No of hits)
miR-17a	2	**Pol(1),** Env/Rem Ex1 (1)
miR-18a	8	**Gag(2), Pol(2),** Env (1), Env/Rem Exon 1 (1), Rem Exon 2/Sag/3' LTR (2)
miR-19b	3	**Gag(1), Pol(1),** Env (1)
miR-20a	15	**Gag(3), Pro(3), Pol(2),** Env (6) 3' LTR (1)
miR-92a	46	**Gag (10), Pro(5), Pol (10),** Env (11), Env/Rem Exon 1 (2), Rem Exon 2/Sag (6), 3' LTR (2)
Total Sites	**74**	Gag (16), Pro(8), Pol (16) = **40 in gRNA**

*The 5' LTR did not show any significant hits according to the set parameters, while any hit in the 3' LTR was common to all mRNAs.

C.

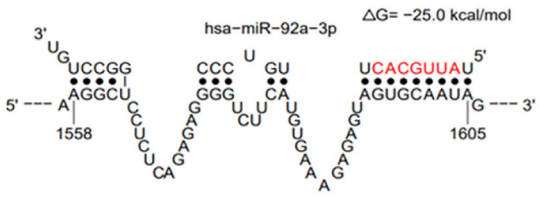

Figure 6. An *in-silico* analysis of the potential of the miR-17-92 cluster members to target the MMTV genomic RNA using STarMir bioinformatic tool. (A) Illustration of the MMTV genome and its various mRNAs along with the potential miR-17-92 cluster member predicted binding sites. The shaded box in blue highlights the region of the MMTV genome exclusively found in the full-length genomic RNA which is the same as the mRNA for Gag/Pro/Pol viral proteins. **(B)** Characterization of the miRNAs predicted to target the MMTV mRNAs. The target RNA regions highlighted in red belong exclusively to the full-length Gag/Pro/Pol mRNA or the genomic RNA (gRNA) with the number of target sites observed in parenthesis. **(C)** Illustration of the highest probable binding site of miR-92a on MMTV Gag.

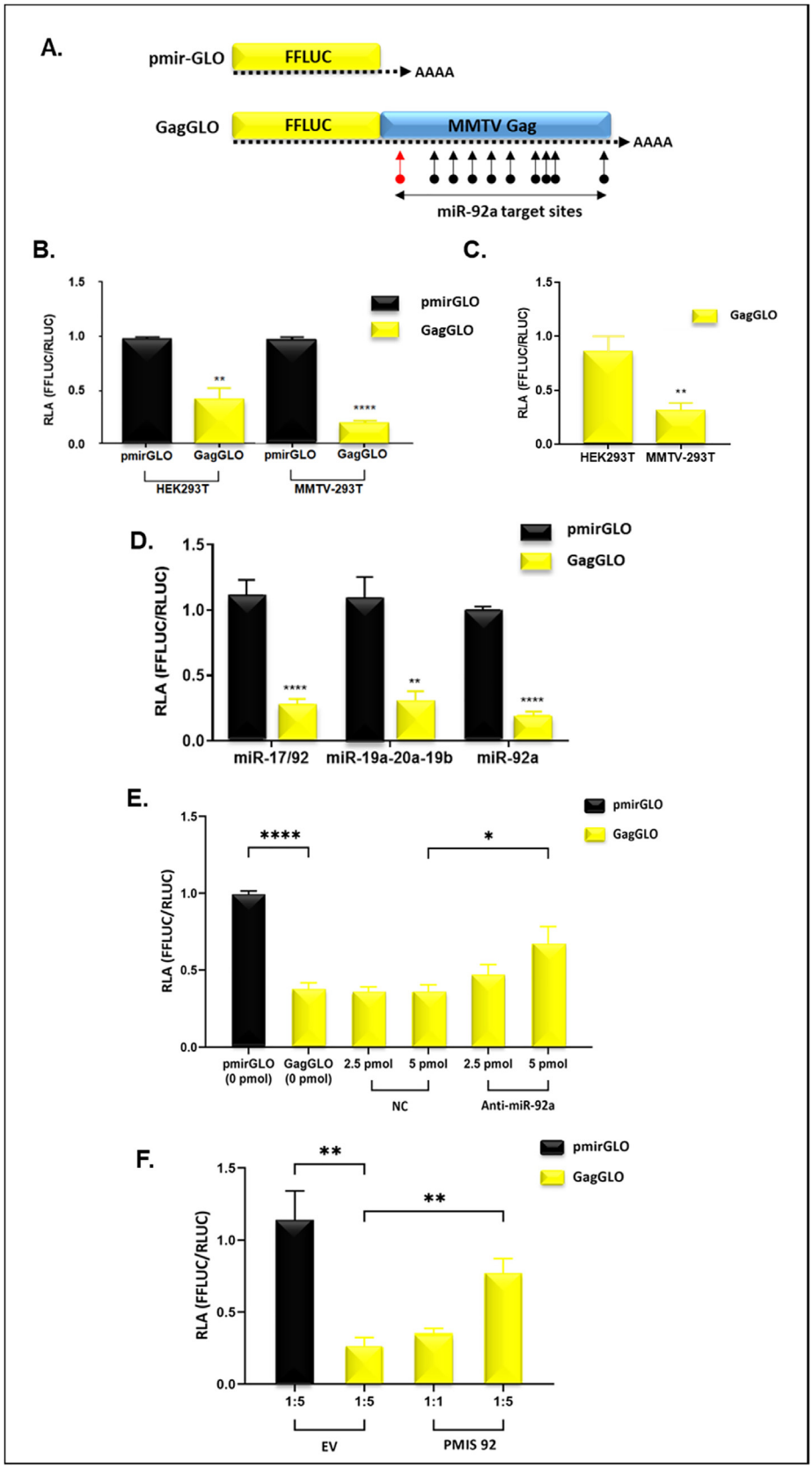
A.
pmir-GLO
FFLUC
AAAA
GagGLO
FFLUC
MMTV Gag
AAAA
miR-92a target sites
B.
RLA (FFLUC/RLUC)
pmirGLO
GagGLO
pmirGLO
GagGLO
pmirGLO
GagGLO
HEK293T
MMTV-293T
C.
RLA (FFLUC/RLUC)
GagGLO
HEK293T
MMTV-293T
D.
RLA (FFLUC/RLUC)
pmirGLO
GagGLO
miR-17/92
miR-19a-20a-19b
miR-92a
E.
RLA (FFLUC/RLUC)
pmirGLO
GagGLO
pmirGLO (0 pmol)
GagGLO (0 pmol)
2.5 pmol
5 pmol
2.5 pmol
5 pmol
NC
Anti-miR-92a
F.
RLA (FFLUC/RLUC)
pmirGLO
GagGLO
1:5
1:5
1:1
1:5
EV
PMIS 92

in transient transfection assays to determine whether presence of enhanced levels of cluster members in the HEK293T-MMTV cells would target the hybrid GagGLO mRNA in the MMTV-expressing cells, resulting in reduction in the luciferase activity compared to its expression in the HEK293T cells devoid of MMTV expression.

As can be seen, the levels of normalized firefly luciferase activity from GagGLO in the HEK293T-MMTV cells was indeed significantly lower compared to its expression in the normal HEK293T cells (Figure 7B). Interestingly, even in the HEK293T cells lacking MMTVs, there was a significant down-regulation of GagGLO, most likely due to the presence of endogenous miRNAs like miR-92a and others that may target the Gag region. The luciferase activity of GagGLO was reduced by 80% in the HEK293T-MMTV cells compared to HEK293T cells, pointing to the potential activation of miR-92a expression in the presence of MMTV (Figure 7C). The same effect was observed when these two vectors were tested in the three cell lines that over-expressed either the whole miR-17-92 cluster, the truncated cluster (miR-19/20), or miR-92a only, thus mimicking MMTV infection which up-regulates miR-92a (Figure 7D). It is critical to note that a specific miRNA-binding site on Gag can only accommodate a single miRNA at any given time,[77] thereby making the target gene susceptible to miRNA-mediated repression regardless of the amount of exogenous miRNA present. This may explain why we did not observe a dose response when anti-miR-92a oligos were used for inhibition (Figure 3H), and luciferase activity was down-regulated to about the same extent across the five cell lines assessed (Figure 7B and D).

Finally, we wanted to confirm that the repression of luciferase activity in the GagGLO cells being observed was indeed due indeed to miR-92a primarily targeting the Gag gene. Therefore, we transfected pmirGLO and GagGLO in HEK293T cells in the presence of anti-sense oligo inhibitors of miR-92a compared to a scrambled control (NC). As can be seen, transfection of the anti-miR-92a oligos led to a dose-dependent rescue of luciferase activity which was statistically significant, a rescue that was not observed in the presence of increasing amounts of the scrambled oligo control (Figure 7E). To further confirm these findings, we tested GagGLO in the presence of our plasmid-based inhibitor against miR-92, PMIS92a, used earlier in Figure 4. Similar to the anti-sense inhibitor oligos, expression of the plasmid-based inhibitor of miR-92a led to a reversal of inhibition of luciferase activity from GagGLO which was also dose dependent and statistically significant (Figure 7F). This reversal was not observed when the control empty vector (EV; i.e., pmirGLO) was used at the higher dosage of 1:5 similar to GagGlo, revealing the specificity of this rescue (Figure 7F). In both instances of rescue with anti-sense oligos or plasmid-based inhibitors, the rescue of luciferase activity was not quite complete and up to about 75–80%. This is probably due to the effect of other cluster members that also putatively target the MMTV genome, such as miR-17, as shown in our present study (Figure 4). Thus, these two independent approaches confirm that miR-92a is the primary member of the cluster that inhibits MMTV by targeting the Gag sequences of the viral genomic RNA.

Together, these results suggest that the Gag region of the MMTV genome, a region that is part of the full-length RNA since it is removed from the various spliced mRNAs of MMTV, is a target of the miR-17-92 cluster members, more specifically miR-92a. While it would be valuable to mutate the predicted functional binding site of miR-92a in the Gag region to definitively confirm our findings, given the other 15 predicted miR-92a binding sites

Figure 7. The miR-92a member of the miR-17-92 cluster targets the MMTV genome. Dual-Luciferase activity-based interaction assays were conducted to test the interaction of the miR-17-92 cluster in general, and miR-92a in particular, with the MMTV genome. **(A)** Illustration of the pmirGLO and GagGLO constructs and the transcripts produced in the presence or absence of the gag *gene* cloned downstream of the *firefly luciferase* gene. The arrows indicate pmiR-92a binding sites with the red arrow showing position of the most probable binding site. The parental pmirGLO control vector also has an internal *renilla luciferase* gene cassette serving as an internal control of transfection efficiency. The over-expression reporter vectors, pmiRGLO (control) & GagGLO were transfected into: **(B)** HEK293T and MMTV-293T cells and dual luciferase activity was determined 48 h post-transfection. **(C)** A re-comparison of relative luciferase activity of GagGLO in HEK293T (control) and MMTV-293T cells shown in panel B. **(D)** Test of the pmirGLO constructs in the three specific miR-17-92 or their derivative overexpressing (OE) cell lines, as described earlier. **(E)** Test of the pmirGLO & GagGLO constructs in the presence of scramble control (NC) and anti-sense oligo inhibitor against miR-92a. **(F)** Test of the pmirGLO & GagGLO constructs in the presence of plasmid-based inhibitor against miR-92a, PMIS92a. Luciferase activity from the empty vector (EV), i.e., was designated as 1 with means represented as ± SD (n = 3). Statistical significance is shown as * where *$p \leq 0.05$; **$p \leq 0.01$, ***$p \leq 0.001$, ****$p \leq 0.0001$.

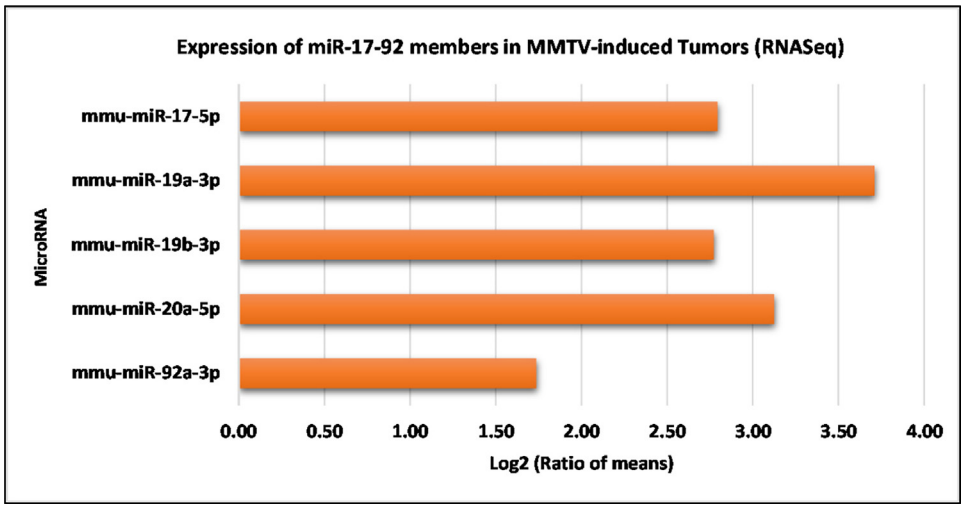

Figure 8. Expression of miR-17-92 cluster members in MMTV-induced tumors. Data representing the mean expression of miR-17-92 cluster members in MMTV-induced tumors (n = 2) and infected mammary glands (n = 2) obtained by small RNAseq analysis.[58]

in Gag that could also be important, this aspect will be explored in future studies in a systematic manner.

miR-92 expression is least among cluster members in MMTV-induced tumors

While these observations explain how the miR-17-92 cluster functions an "anti-viral" response to suppress MMTV replication in cell lines, they do not explain our observation of high levels of MMTV expression in the presence of up-regulation of the miR-17-92 cluster members in both the infected mammary glands and mammary tumors of MMTV-infected mice.[58] We speculate that upon initial MMTV infection, the cells mount an anti-viral response to suppress MMTV infection by activating the miR-17-92 cluster, and in particular miR-92a. However, the virus is able to overcome this restriction by subverting the expression of miR-92a, leading to enhanced virus expression that eventually leads to mammary tumorigenesis. This speculation suggests that the elevated levels of MMTV in mammary tumors, despite the up-regulation of some cluster members, could be due to lower levels of miR-92a expression in the tumor samples.

To test this hypothesis, retrospection into the small RNAseq data from MMTV-induced tumors conducted earlier[58] revealed interesting expression patterns of the miR-17-92 cluster members which further gives confidence to our assertion. Intriguingly, while an increased expression of the oncogenic miR-17-92 family members (miR-17, miR-19a, miR-19b, & miR-20a), could be observed,[41] the expression of miR-92a was the least amongst the expressed cluster members (Figure 8). This suggests that the major anti-viral component of the miR-17-92 cluster was suppressed in MMTV-induced mammary tumors compared to uninfected mammary glands, observations that need to be investigated further to support our developing hypothesis.

Discussion

The current study stemmed from our observations that MMTV disrupts expression of host miR-17-92 cluster in mice,[58] suggesting a possible interaction between the cluster and the virus to facilitate virus replication and presumably tumor induction. Using functional assays that manipulated endogenous levels of miR-17-92 (Figures 1–4) as well as mutational analysis (Figure 5), we identify an anti-viral role of the miR-17-92 cluster in MMTV replication where the cluster member, miR-92a, was observed to target the full-length MMTV genomic RNA, thereby drastically suppressing MMTV replication (Figures 6 and 7). Thus, the miR-17-92 cluster, and especially miR-92a, acts as part of the cell's anti-viral response, thwarting incoming virus infections for which miRNAs are well known for.[19,20,22] However, MMTV overcomes this suppression with time, to induce the more oncogenic cluster members, as observed in the tumor environment (Figure 8).

Context-dependent expression & structure of miR-17-92 cluster

A similar expression profile has been frequently demonstrated in different sub-types of breast cancer, with various members of the cluster, and especially miR-17, miR-19 and miR-20, implicated

in tumor induction and/or progression.[78,41] The expression of miRNA cluster members is tightly controlled in a cell, cluster, and context-dependent manner where the type of *trans* factors (proteins & long non-coding RNAs), the diseased state of the cell, the position of the member within the cluster, and the tertiary structure of the cluster, are all are intricately involved in this regulation.[35] Our findings in mammary tumors supports the tertiary structure model of the pri-miR-17-92 having a dense super-coiled core rendering miR-92a being the least accessible by the microprocessor complex.[79] This contrasts with another model in which miR-92a is the most accessible member for initial processing.[80] These models suggest that miR-17-92 cluster may adopt a different three-dimensional structure in infected mammary epithelial cells, facilitating the expression of miR-92a, but different from that of the primary breast tumors in which its structure may be inhibiting miR-92a expression, an aspect that warrants further study in mice.

Virus infections and the miR-17-92 cluster

Differential regulation of miR-17-92 cluster members by viral infections has significant pathological implications. For instance, RSV-infected infants show reduced levels of miR-92a and increased levels of miR-20a and paralogue miR-106b-5p, implying their roles in immune regulation of RSV infections.[81] As mentioned earlier, miR-92a has complex, cell context-dependent roles. In B-cell lymphomas driven by an aberrant expression of c-Myc, miR-92a neutralizes miR-19′s tumorigenic effect by stabilizing c-Myc.[82] With the acquisition of p53 mutations, impairment of the delicate balance between miR-92a and miR-19 levels is thought to foster the establishment of these c-Myc-induced tumors. Similarly, we observed an unexpected down-regulation of miR-19a in the miR-19/20 OE cell line (Figure 2E) likely due to the reported antagonistic interactions between the miR-19 family and miR-92a.[83,82] The significant up-regulation of miR-92a in HEK293T-MMTV-miR-19/20 OE cell line (Figure 2E) may affect miR-19a levels, potentially explaining the observed down-regulation of MMTV Gag (Figure 2G and H), despite the lack of over-expression of the tested miRNAs (Figure 2D).

miR-92a-mediated repression of MMTV

It is well known that expression levels of individual mature cluster members varies, depending upon the infectious agent.[84,85,37] In our MMTV-expressing HEK293T cells, miR-92a expression significantly increased, while other members, like miR-17 and miR-19a, were less affected (Figure 1B). Interestingly, over-expression of the miR-17-92 cluster in these cells led to a similar observation with relatively the same expression profile of miR-17, but an up-regulation of miR-19a by ~8-folds and miR-92a by ~250-folds (Figure 2D). In fact, miR-92a remained the highest expressed member in all the three OE cell lines (Figure 2D–F), which is presumably what led to the down-regulation of MMTV Gag expression in these cell lines (Figure 2G), equivalent to the levels observed in miR-92a expressing cells alone (Figure 2I and H). This was further validated by inhibiting miR-92a that relieved this suppression, independent of the approach used (Figures 3 and 4), including mutational analysis where the miR-92a seed sequence was either substituted or deleted (Figure 5). Finally, one of the regions of the MMTV genome targeted by the cluster- Gag, was identified as a direct target of miR-92a using dual luciferase assays (Figures 6 and 7). These data reveal that miR-92a is the critical component of the cluster that suppresses MMTV expression.

Oligo-based inhibition of individual cluster members and compensatory effects of other members

By independently suppressing distinct members of the miR-17-92 cluster, miR-17, miR-19a, and miR-92a, we established that inhibiting these miRNAs could restore MMTV gene expression (Figure 3). This was achieved in our three miRNA overexpression cell lines by employing anti-miR inhibitors specific for each miRNA, while a combinatorial approach was used in the miR-17-92 OE cell line. miRNA inhibitors block mature miRNAs from binding to their targets.[86] Interestingly, while we observed a statistically significant increase in MMTV genomic RNA expression (Figure 3E) and a modest rescue in Gag protein expression (Figure 3D) after cluster inhibition, individual miRNA inhibition was unsuccessful at the miRNA level (Figure 3A). The lack of significant inhibition of target miRNAs in miR-17-92 OE and miR-19/20 OE cell lines (Figure 3A and B) is probably due to compensatory effects by other cluster members. The notable inhibition of miR-92a in miR-92a OE cells (Figure 3C) supports this notion since miR-92a does not share its seed sequence with any other member of the cluster.[73,74] Since the repressive miRNAs were inhibited, no significant variation was observed in genomic RNA levels between the miR-19/20 and miR-92a OE cell lines when compared to the control (Figure 3F and G). However, a statistically significant increase in MMTV genomic RNA expression was observed in miR-17-92 OE cells (Figure 3E). We speculate that the miR-92a suppression of MMTV in miR-17-92 OE cells is removed upon the addition of the anti-miR cocktail that contains 15 pmol of anti-miR-92, even though the reduction in miR-92a was statistically non-significant (Figure 3A). As seen earlier in Figure 2D, we know that miR-92a is highly expressed in this cell line, thereby the inhibitor, even if active partially, relieves this suppression to a minor extent which was reflected at the genomic RNA level (Figure 3E).

This was confirmed by a significant rescue of MMTV gene expression upon inhibiting miR-92a at various dosages (Figure 3H). A considerably better rescue was observed at 15 pmol of inhibitor than at 45 or 60 pmol due to possible saturation of the miRNA binding sites. This notion is in agreement with the work of Mayya and Duchaine who demonstrated that only a small fraction of miRNAs, determined by a combination of expression threshold, miRISC abundance, and low target site availability, are vulnerable to competitive effects via miRNA-binding sites.[87] However, the role of other cluster members in modulating MMTV replication needs to be explored further since they share seed sequences which may alter their individual effect by collaborative interactions among themselves.

This raises the question of how these miRNAs may be affecting Gag protein expression. We speculate that this may be due to the effect of miRNAs targeting Gag mRNA translation. Since miRNAs are known to target mRNA at both the RNA (through deadenylation/decapping of mRNA) and protein levels (translational inhibition through formation of biomolecular condensates),[88,89] we believe the phenotype observed for the anti-sense oligo results could be attributed to the removal of translational repression of MMTV gene expression.

Quirks of the plasmid-based inhibition of cluster members

Using plasmid-based inhibitor vectors, we validated our findings in cell lines stably expressing anti-miRNAs against miR-17 and miR-92a (Figure 4). Although these PMIS cell lines did not significantly inhibit target miRNAs (Figures 4A and B), MMTV expression increased significantly at both the protein and RNA levels, respectively (Figures 4D and E). We believe that the limited inhibition of miR-92a levels by PMIS 92 is likely due to the inability of the PMIS system to reduce the high levels of miR-92a previously demonstrated in Figure 1E, as supported by the antisense oligo-based inhibition experiment (Figure 3). Despite this, partial inhibition of miR-92a by the PMIS system improved MMTV Gag expression compared to the control EV cell line. We further confirmed this by examining the downstream effect of PMIS 17 on the target PTEN levels in the PMIS 17-expressing stable cell line (Figure 4B). The mechanism of PMIS-based inhibition involves forming stable complexes with mature miRNAs through antisense sequences that are flanked by engineered stem loops, preventing their interaction with mRNA targets and leading to gene expression inhibition.[72] The flanking hairpins recruit the same proteins to this complex that facilitate formation of RISC, such as Dicer, Argonaute, TRBP, and others. However, while Dicer dissociates from the mature miRNA-anti-sense miRNA complex, the other proteins remain associated, forming a stable complex that prevents the mature miRNA from interacting with its mRNA target and leads to its degradation, inhibiting specific gene expression.[72]

In the PMIS 92 cell line, we observed an up-regulation of miR-92a rather than its inhibition (Figure 4A). This unexpected result is likely due to significant expression of anti-miRNA molecules being converted into cDNA and measured alongside miRNAs in RT-qPCR reactions.[90] Thus, despite the inability to show a physical down-regulation of the targeted miRNAs via PMIS using RT-qPCR assays, we demonstrate a functional inhibition of miR-17 and miR-92a, as observed by a substantial rescue of MMTV Gag at both the RNA and protein levels (Figure 4D and E). Based on the results presented in Figures 3 and 4, we demonstrate that miR-92a is a powerful anti-viral component that by itself lowers MMTV gene expression to the same level as the entire cluster.

Potential activators of miR-17-92 cluster upon MMTV expression

These findings raise the question of how the miR-17-92 cluster is activated upon MMTV infection. Literature reports transcription factors and cell cycle regulators, such as Myc, Stat3, Ccnd1, and members of the E2f family, such as E2f-1 and E2f-3 play a role in regulating the cluster expression.[91,39,92–94] Our mRNAseq data from MMTV-expressing HC11 cells[95] point to the potential role of c-Myc in this process which had a ~3-fold induction in expression in the presence of MMTV, while a ~2-fold down-regulation of Ccnd1 was also observed, a regulator of cell cycle. These observations suggest that c-Myc may be one of the factors involved in the activation of the miR-17-92 cluster in our system (Table 1). Further experiments are needed to validate which factor(s) is/are involved in this activation.

Working model

Based on the results presented, this study suggests a negative regulatory interaction between the host miR-17-92 cluster and MMTV. We postulate that MMTV infection activates the miR-17-92 cluster, leading to up-regulation of miR-92a which targets the MMTV genomic RNA and downregulates MMTV Gag/Pro/Pol expression and virus production (Figure 9). Thus, this study provides the first evidence of miRNAs modulating MMTV replication in a biologically relevant manner. Interestingly, miR-92a was found at lower levels in MMTV-induced breast tumors, suggesting that MMTV subverts miR-92a expression to enhance viral replication during tumorigenesis. This down-regulation in infected mammary glands and tumors indicates that MMTV disrupts miR-92a regulation, possibly by altering the cluster's tertiary structure, contributing to tumor development. This highlights a novel mechanism of tumorigenesis beyond

Table 1 Expression of miR-17-92 cluster activators in HC11-MMTV cells using RNAseq.

S No.	Activators of miR-17-92	Fold Change (Log2)
1	**Myc***	**2.95**
2	Stat3	0.41
3	**Ccnd1***	**−1.92**
4	E2f1	−0.27
5	E2f2	−0.51
6	E2f3	0.78
7	p65/RELA	0.57

* Genes dysregulated in a significant manner.

traditional insertional mutagenesis, an aspect that needs to be explored further experimentally.

While this study establishes the anti-viral role of the miR-17-92 cluster against MMTV, it raises important questions for future research into virus-host interactions. For example, how the different members of the miR-17-92 cluster and MMTV interact with each other to facilitate the anti-viral phenotype observed. With six mature miRNAs orchestrating a plethora of regulatory functions in a cell, an in-depth analysis of effector proteins regulated in MMTV infection should help us better define the pathways and their functional consequences in the MMTV life cycle. It is also important to understand whether MMTV is a regulator of miR-17-92 cluster alongside other potential cellular activators and what the physiological role of miR-92a-medicated regulation of MMTV is *in vivo*, especially its relevance to tumorigenesis.

Significance

MMTV is a non-acute, slow-transforming retrovirus that primarily causes breast cancer but also lymphomas/leukemia in mice. Consequently, understanding how MMTV interacts with its host can offer critical insights into cellular anti-viral responses and the process of tumorigenesis. Our study indicates that the host miR-17-92 cluster

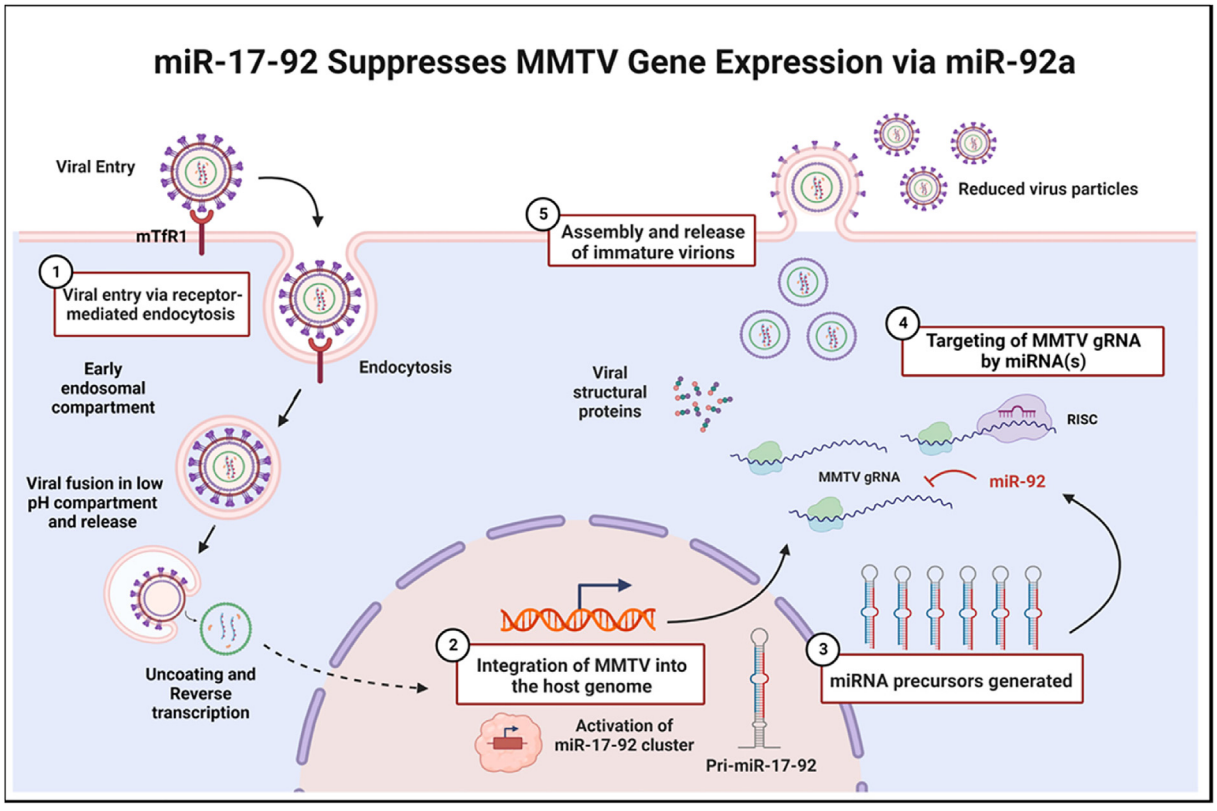

Figure 9. Schematic representation of model representing miR-17-92-mediated regulation of MMTV gene expression. MMTV entry via murine transferrin receptor 1 (mTfR1) is followed by fusion of the viral capsid in a late endosomal compartment under low pH, uncoating/reverse transcription, and integration of the viral genome into the host chromosome. The cellular/viral factor-assisted transcriptional activation of the miR-17-92 cluster leads to up-regulation of the pri-miR-17-92. Once activated, due to the differential processing of the cluster, there is an increase in the expression levels of the mature miR-92a cluster member, which in turn, targets the MMTV unspliced genomic RNA. With more than 10 statistically significant miR-92a binding sites on the viral *gag* region, down-regulation of the genomic RNA takes place, resulting in suppression of MMTV replication. This is because the unspliced genomic RNA serves as the mRNA for the translation of the viral structural and enzymatic proteins (Gag/Pro/Pol) as well as the source of genomic RNA for encapsidation into the newly forming viral particles.Illustration created on *BioRender.*

acts as an anti-viral agent during MMTV infection, but is counteracted by MMTV during tumorigenesis. This observation is significant since MMTV-induced tumors share similarity with human breast cancer, making the MMTV/mouse model crucial for studying breast cancer initiation, progression, and therapy. Therefore, understanding how hosts use miRNAs to inhibit MMTV replication and how the virus evades this response during tumorigenesis can contribute to a better understanding of human breast cancer.

Materials and Methods

Nucleotide numbering

All nucleotide numbers in this study refer to the nucleotide positions of the exogenous C3H proviral strain of MMTV that is 9,895 bp in length (GenBank accession number AF228552).

Cell lines and culture conditions

The HEK293T cells were cultured in Dulbecco's modified Eagle's medium, DMEM (HyClone, USA), which included 10% fetal bovine serum (HyClone Laboratories Inc., Logan, UT USA). All cell lines had their culture medium supplemented with 1% penicillin and streptomycin (10,000 g/ml; Life Technologies, Carlsbad, CA USA), as well as 0.1% gentamicin (50 mg/ml; Life Technologies, USA). All cell lines were maintained at 37 °C and 5% CO_2 inside a water-jacketed incubator (Forma-series II, Thermo Fisher Scientific, USA). HC11 cell culture has been described before.[94]

MMTV stable cell lines

An HEK293T stable cell line that constitutively expressed MMTV was established using HYBMTV, a molecular clone of MMTV that is capable of infection and tumorigenesis.[70] The cells were transfected with linearized HYBMTV plasmid using Lipofectamine 3000 (Invitrogen, Thermo Fisher Scientific, USA) according to manufacturer's instructions. After a period of 48 h post transfection, the HEK293T-MMTV stable cells were selected for positive clones in hygromycin selection media (200 μg/ml). After four weeks of selection, the isolated colonies were tested for the expression of MMTV Gag by western blotting analysis. The HEK293T (control) cell line was maintained in DMEM and the established HEK293T-MMTV stables were maintained in DMEM- media containing hygromycin (200 μg/ml). All MMTV expressing cell lines were treated with $10^{-}6$ M Dexamethasone (Sigma-Aldrich, Saint Louis, MI USA) 8 h prior to harvesting to increase MMTV gene expression through hormonal stimulation of its promoter.[96] HC11 cells expressing HYBMTV stably have been described before.[95]

Plasmids

The miRNA over-expression plasmids and miR-92a mutation/deletion plasmids were obtained from Addgene vector repository, USA (Table 2). The Dual luciferase miRNA target vector (pmirGLO) was purchased from Promega, Madison, WI, USA. The AK14 plasmid used for the construction of the MMTV Gag-containing dual luciferase construct, GagGLO, has been described before.[68] To test the miR17-92 cluster target sites predicted within Gag, the MMTV Gag expression plasmid, AK14, was digested with *Xho*I to obtain the complete MMTV Gag region (nt 1485- nt 3258). The *gag* gene was then cloned into the *Xho*I site downstream of the *firefly luciferase* gene of pmirGLO to create the Gag target vector, GagGLO. All constructs used in the study were verified by restriction enzyme digestion and sequencing, and are listed in Table 2.

miRNA over-expression and inhibition experiments

For miRNA over-expression or plasmid-based inhibition analysis, the HEK293T-MMTV cells were transfected with the appropriate plasmids (listed in Table 2) using Lipofectamine 3000 (Invitrogen,

Table 2 List of plasmids used in this study.

Plasmid	Function	Source	Reference
MSCV	Empty vector control with GFP and puromycin selectable markers	Addgene (#24828)	103
MSCV-miR-17-92	MSCV vector expressing wild type miR-17-92 cluster	Addgene (#64100)	82
MSCV-miR-19a-20a-19b	MSCV vector expressing miR-19a, miR-20a and miR-19b of the cluster	Addgene (#24827)	103
MSCV-miR-92a	MSCV vector expressing miR-92a of the cluster	Addgene (#64092)	103
PMIS NC	Control vector with scramble oligo	NaturemiRI	72
PMIS17	PMIS vector expressing anti-miR-17	NaturemiRI	72
PMIS92a	PMIS vector expressing anti-miR-92a	NaturemiRI	72
MLS-miR-17-92a	MLS vector expressing wild type miR-17-92 cluster	Addgene (#64090)	103
MLS-miR-17-19b	MLS vector expressing truncated miR-17-19b cluster w/o miR-92a	Addgene (t#64089)	103
miR-17-92aMUT	MLS vector expressing miR-17-92 cluster w/ mutated miR-92a	Addgene (#64094)	82
AK14	Gag expression vector	Tahir A. Rizvi	68

Thermo Fisher Scientific, USA), as described by the manufacturer. Briefly, 5×10^5 cells were plated per well of a 12-well plate the day before transfection. The plasmid DNA (3 μg/well) was added to the DNA/lipid cocktail, followed by incubation for 15 min at room temperature. The mixture was added to the cells dropwise while swirling. The transfected cells were returned to the incubator and inspected for GFP positive cells at the 48-hour time point. If positive, they were selected in 3 μg/ml puromycin or another appropriate antibiotic selection media for 5 or more days for stable selection.

To prepare viral particles, cell supernatant was pre-cleared by low-speed centrifugation followed by filtering through a 0.2 μm filter. Virus particles from the clarified cell supernatants were purified by ultra-centrifugation at 26,000 rpm using the SW50.1 rotor for 90 min through a 2 ml, 20% sucrose cushion. The viral pellets obtained were then scrapped into 300 μl of 1 × TNE buffer (1 mM EDTA, 10 mM Tris–HCl of pH 7.5, 100 mM NaCl) and divided for RNA and protein analyses.

miRNA inhibition experiments using Anti-miR oligos

Functional inhibition of miRNAs in the cluster was achieved using the potent mirVana oligo-based inhibitors for miR-17, miR-19a and miR-92a (Thermo Fisher Scientific, USA): miR-17 (MIMAT0000070), miR-19a (MIMAT0000073), and miR-92a (MIMAT0000092) along with negative control (NEG#1 Cat.No:4464076). The oligo inhibitors were resuspended in nuclease free water to make 100 μM inhibitor stock solution, according to the manufacturer's protocol. Inhibitors (alongside a negative scramble control) were used at a final concentration of 15 pmol/well and were transfected into the specific over-expression cell line using Lipofectamine 3000. A combination of miR-17, miR-19, and miR-92a inhibitors (15 pmol/inhibitor each) was used to treat the complete miR-17-92 cluster over-expression cell line with the intention of inhibiting the three miRNAs in the cell line simultaneously. The treated cells were harvested 72 h post transfection and processed for RNA and protein for further analysis.

RNA sequencing (mRNAseq and miRNAseq)

Total cellular RNA was extracted from normal mouse mammary epithelial HC11 cells or HC11 cells expressing MMTV, HC11-MMTV, using the TRIzol Reagent (Invitrogen, Thermo Fisher Scientific, Waltham, MA USA). Whole cell RNA was sequenced for both mRNA and miRNA expression from two independent biological replicates of the HC11 and HC11-MMTV cell lines using the TruSeq library-NovaSeq6000 platform (for mRNAseq) or TruSeq SBS KIT-HS V3-HiSeq 2000 system (for small RNAseq) commercially by the Beijing Genomics Institute (BGI, Hong Kong). Data analysis was carried out using BGI's online tool, Dr. Tom. The validated mRNAseq data has already been published.[95]

RNA extraction and cDNA synthesis

RNA was extracted from cells and viral particles using the Trizol Reagent (Thermo Fisher Scientific, USA) and quantified using a Nanodrop spectrophotometer. To ensure DNA-free preparations, 6 μg of the extracted RNA was DNase-treated for 30 min at 37 °C with 2 units (U) of Turbo DNase I (Invitrogen, Thermo Fisher Scientific, USA) along with 40 units of Recombinant RNasin (Promega, USA). After confirmation of DNA free preparations using PCR, the RNA was further reverse transcribed to cDNA using MMLV-RT (Promega, USA) and used for downstream mRNA qPCR assays. For miRNA quantification, 10 ng of isolated total RNA was converted into cDNA using the TaqMan™ miRNA Reverse Transcription Kit (Applied Biosystems, Foster City, CA, USA) which was subsequently used for stem-loop-based real time PCR using TaqMan® miRNA Individual Assays and the TaqMan® Universal PCR Master Mix with AmpErase® UNG (Applied Biosystems, USA).[97]

Quantitation of MMTV by real-time PCR

Real-time quantitation of MMTV full length genomic and all mRNAs was performed using customized TaqMan assays (FAM-labelled).[66,67] Briefly, all MMTV mRNAs were quantified using an assay specific for the 5′ U5 region within the HYB-MTV genome (nt 1192–1259) and genomic RNA was quantified using an assay that targeted the nucleotide region 1729–1791 of MMTV *gag*. The experiments were normalized using human β-Actin as the endogenous control (FAM/MGB probe, cat. no. 401846; Applied Biosystems, USA).

Quantitation of Pri-miRNAs by SYBR Green qPCR

The pri-form of miR-17-92 cluster was quantified using SYBR Green qPCR assay utilizing 5X HOT FIREPol® EvaGreen® qPCR Mix (Solis BioDyne, Estonia) with two individual primer sets described earlier[98,99] that were renamed OFM 450/451, OFM 446/447 in this study. The amplification reaction contained template nucleic acid (1 μl of cDNA), 4 μl 5X HOT FIREPol® EvaGreen® qPCR mix, 0.8 μl per Primer (400 nM), and nuclease-free water in a total reaction volume of 20 μl. The qPCRs were performed in triplicates under the following cycling conditions: 50 °C for 2 mins, initial denaturation at 95 °C for 12 mins, 40 cycles of 95 °C for 15 secs, annealing at 60 °C for 30 secs, extension 72 °C for 30 secs,

and a final extension at 72 °C for 10 min. The primers used for the assays are listed in Table 3.

Quantitation of mature miRNAs by TaqMan assays

The mature miRNA species were quantified using the previously-validated TaqMan miRNA assays for miR-17 (Assay ID: 002308), miR-19a (Assay ID: 000395) and miR-92a (Assay ID: 000430) (Applied Biosystems, USA), as per manufacturer's protocol. The experiment was normalized using U6 snRNA (Assay ID: 001973) as the endogenous small RNA control. The assays were carried out in a volume of 20 μl in triplicates using QuantStudio™7 Flex Real-Time PCR System following the standard conditions: 2 min at 50 °C, 10 min at 95 °C for denaturation, followed by 40 cycles of denaturation at 94 °C for 15 s and annealing/extension for 1 min at 60 °C. The data was analyzed using the $2^{-\Delta\Delta Ct}$ method.[100]

Western blotting

Whole cell extracts and virus particles were analyzed by western blotting to quantify MMTV protein expression. Harvested cells were lysed in RIPA buffer [1 mM EDTA, 10 mM Tris–HCl (pH 8.0), 0.1% sodium deoxycholate, 1% Triton X-100,140 mM NaCl and 0.1% SDS] supplemented with 50 μl β-mercaptoethanol and 1 mM PMSF (Sigma-Aldrich, USA) per ml of RIPA buffer. For the analysis of extracellular viral particles, a volume of 50 μl of 1X TNE solution was used to resuspended the virions pellet by ultracentrifugation followed by addition of the 6x SDS loading buffer to 1x and SDS-PAGE separation. Extracted cellular proteins were quantified using the Bradford Reagent (Bio-Rad Laboratories, Hercules, CA USA) as per manufacturer's directions. Subsequently, lysates were separated on 4–12% SDS polyacrylamide gels and transferred overnight at 4 °C, 30 V or at 90 min, 90 V onto nitrocellulose membranes (GE Healthcare, Chicago, IL USA). The blocked membranes were probed with either rabbit polyclonal MMTV anti-Gag antibody (Rockland Immunochemicals, Inc, Limerick, PA USA) at a dilution of 1:1000 in 2% non-fat dry milk overnight at 4 °C, or anti-GAPDH followed by a 1-hour incubation at room temperature with the appropriate secondary antibody conjugated with horseradish peroxidase. The chemiluminescent signal was detected using the ECL Plus Western blotting substrate or SuperSignal™ West Femto Maximum Sensitivity Substrate (Thermo Fischer Scientific, USA), as directed by the manufacturer, and captured using the TyphoonFLA9500 (GE Healthcare, USA) or an X-ray film. GelQuantNET software was employed for densitometric analysis.

Dual luciferase assays

For miRNA target analysis, HEK293T and HEK293T-MMTV cell lines over-expressing miR-17-92, miR-19a/20a, and miR-92a, or HC11 cells (1×10^5 cells in 24-well plates) were transfected with the Dual Luciferase constructs- pmirGLO or the MMTV-GAG containing, GagGLO using Lipofectamine 3000, as described by the manufacturer. The cells were harvested 48 h post transfection, and whole cell lysates prepared and assayed for luciferase activity using the Dual Luciferase Assay System as per manufacturer's directions (Promega, USA). The luminescence signal was detected using the Promega GloMax luminometer. The Firefly luciferase activity was normalized to Renilla luciferase expression and expressed relative to the experimental control, pmirGLO. All assays were conducted in triplicates and independently repeated two times.

miRNA-mRNA target prediction

All potential miR-17-92 binding sites on the MMTV genome were predicted using Sfold StarMirDB web server for miRNAs: (https://sfold.wadsworth.org/starmirDB.php).[101,102] The following parameters were followed through the bioinformatic analysis: Logistic probability >0.75, ΔGHybrid ≤ -20 kcal/mol, Preferential Seed type − 8mer/7mer.[76]

Statistical analysis

Statistical analysis was performed using GraphPad Prism Version 7.0. Statistical significance was determined using the paired student's *t* test, as the mean ± SD. All recorded data in this study were acquired from at least 2

Table 3 Primers used to quantify pri-miR-17-92 and the endogenous control β-Actin.

Primer Name	Primer sequence 3′–5′ (F/R)	Target	Comments
OFM 446	GGGAAACTCAAACCCCTTTCTAC (F)	Pri-miR-17/92	**Primer set 1**[98]
OFM 447	CAACAGGCCGGGACAAGT (R)		
OFM 450	CTGTCG CCCAATCAAACTG (F)	Pri-miR-17/92	**Primer set 2**[99]
OFM 451	GTCACAATCCCCACCAAAC (R)		
β-Actin F	GGGCATCCTGACCCTCAAG	β-Actin	**H_ACTB_1**
β-Actin R	TCCATGTCGTCCCAGTTGGT		(Sigma-Aldrich)

independent experiments. A p value of 0.05 was considered to be least significant where *p is $\leq$0.05; **$p \leq 0.01$, ***$p \leq 0.001$, ****$p \leq 0.0001$. ns (not significant), $p > 0.05$.

To determine significance between groups in small RNAseq data, Q value was estimated which is basically the p value adjusted for the false discovery rate (FDR) using the multiple hypothesis test. The closer the Q value is to zero, the more significant is the data (log2 ratio in our case) between two groups.

CRediT authorship contribution statement

Jasmin Baby: Writing – review & editing, Writing – original draft, Visualization, Validation, Software, Methodology, Investigation, Formal analysis, Data curation, Conceptualization. **Bushra Gull:** Software, Methodology, Investigation, Formal analysis, Data curation, Conceptualization. **Waqar Ahmad:** Visualization, Validation, Software, Methodology, Investigation, Formal analysis, Data curation. **Hala Abdul Baki:** Methodology, Investigation. **Thanumol Abdul Khader:** Methodology, Investigation. **Neena G. Panicker:** Methodology, Investigation. **Shaima Akhlaq:** Methodology, Investigation. **Tahir A. Rizvi:** Writing – review & editing, Resources, Funding acquisition. **Farah Mustafa:** Writing – review & editing, Visualization, Supervision, Resources, Project administration, Funding acquisition, Conceptualization.

DECLARATION OF COMPETING INTEREST

The authors declare that they have no known competing financial interests or personal relationships that could have appeared to influence the work reported in this paper.

Acknowledgments

We would like to thank Prof. Jeffery M. Rosen, Baylor College of Medicine, Houston, TX USA for the gift of HC11 cells, and the Lin He Lab (Lin He, Professor of Cell Biology, Development & Physiology University of California, Berkeley CA, USA) for sharing the miRNA overexpression plasmids: MSCV, MSCV-mir-17-92, MSCV-19a-20-19b, MSCV-mir-92, MLS-mir-17-92, MLS- mir-17-19b, MLS-mir-17-92-Mut92 (Addgene plasmid #: 24828, 64100, 24827, 64092, 64090, 64089, & 64094). We are also grateful to the Amendt Lab (Prof. Brad A. Amendt, Department of Anatomy & Cell Biology, Carver College of Medicine, University of Iowa, Iowa City, IA USA) for providing the PMIS miRNA inhibitor vectors.

Source of funding

This project was supported in part by funds to FM from the College of Medicine & Health Sciences (CMHS), UAE University (UAEU) (grant #12M092), UAEU Zayed Center for Health Sciences (ZCHS) (grant #31R140), Sheikh Hamdan Bin Rashid Al Maktoum Award for Medical Sciences (grant #21M166), and the Al Jalila Foundation (grant #AJF2020006). Research in TAR's laboratory is funded by UAEU Program for Advanced Research (UPAR) (grant #12M103), CMHS, UAEU (grant #NP-24-09; 12M172), Abu Dhabi Department of Education and Knowledge (ADEK) ASPIRE (grant #AARE20-344), and by ASPIRE, the technology program management pillar of Abu Dhabi's Advanced Technology Research Council (ATRC), via ASPIRE "Abu Dhabi Precision Medicine ARI" (grant #VRI-2010).

Appendix A. Supplementary material

Supplementary material to this article can be found online at https://doi.org/10.1016/j.jmb.2024.168738.

Received 15 February 2024;
Accepted 1 August 2024;
Available online 06 August 2024

Keywords:
MMTV;
breast cancer;
miRNAs;
miR-17-92 cluster;
OncomiR-1

† Present address: Department of Microbiology & Immunology The University of British Columbia, Vancouver Campus, Canada.

References

1. Le Grice, S.F.J., (2012). Human immunodeficiency virus reverse transcriptase: 25 years of research, drug discovery, and promise. *J. Biol. Chem.* **287**, 40850–40857. https://doi.org/10.1074/jbc.R112.389056.
2. Perzova, R., Abbott, L., Benz, P., Landas, S., Khan, S., Glaser, J., et al., (2017). Is MMTV associated with human breast cancer? Maybe, but probably not. *Virol. J.* **14**, 196.
3. Amarante, M.K., de Sousa Pereira, N., Vitiello, G.A.F., Watanabe, M.A.E., (2019). Involvement of a mouse mammary tumor virus (MMTV) homologue in human breast cancer: Evidence for, against and possible causes of controversies. *Microb. Pathog.* **130**, 283–294. https://doi.org/10.1016/j.micpath.2019.03.021.
4. Bevilacqua, G., (2022). The viral origin of human breast cancer: From the mouse mammary tumor virus (MMTV) to the human betaretrovirus (HBRV). *Viruses* **14**, https://doi.org/10.3390/v14081704 8.
5. Parisi, F., Freer, G., Mazzanti, C.M., Pistello, M., Poli, A., (2022). Mouse mammary tumor virus (MMTV) and MMTV-

like viruses: An in-depth look at a controversial issue. *Viruses* **14**, 977. https://doi.org/10.3390/v14050977.
6. Dudley, J.P., Golovkina, T.V., Ross, S.R., (2016). Lessons Learned from mouse mammary tumor virus in animal models. *ILAR J.* **57**, 12–23. https://doi.org/10.1093/ilar/ilv044.
7. Ross, S.R., (2010). Mouse mammary tumor virus molecular biology and oncogenesis. *Viruses* **2**, https://doi.org/10.3390/v2092000 9.
8. Hook, L.M., Agafonova, Y., Ross, S.R., Turner, S.J., Golovkina, T.V., (2000). Genetics of mouse mammary tumor virus-induced mammary tumors: Linkage of tumor induction to the gagGene. *J. Virol.* **74**, 8876–8883. https://doi.org/10.1128/JVI.74.19.8876-8883.2000.
9. Katz, E., Lareef, M.H., Rassa, J.C., Grande, S.M., King, L. B., Russo, J., Ross, S.R., Monroe, J.G., (2005). MMTV Env encodes an ITAM responsible for transformation of mammary epithelial cells in three-dimensional culture. *J. Exp. Med.* **201**, 431–439. https://doi.org/10.1084/jem.20041471.
10. Ross, S.R., Schmidt, J.W., Katz, E., Cappelli, L., Hultine, S., Gimotty, P., Monroe, J.G., (2006). An immunoreceptor tyrosine activation motif in the mouse mammary tumor virus envelope protein plays a role in virus-induced mammary tumors. *J. Virol.* **80**, 9000–9008. https://doi.org/10.1128/JVI.00788-06.
11. Swanson, I., Jude, B.A., Zhang, A.R., Pucker, A., Smith, Z.E., Golovkina, T.V., (2006). Sequences within the gag gene of mouse mammary tumor virus needed for mammary gland cell transformation. *J. Virol.* **80**, 3215–3224. https://doi.org/10.1128/JVI.80.7.3215-3224.2006.
12. Flynt, A.S., Lai, E.C., (2008). Biological principles of microRNA-mediated regulation: Shared themes amid diversity. *Nature Rev. Genet.* **9**, 831–842. https://doi.org/10.1038/nrg2455.
13. Nilsen, T.W., (2007). Mechanisms of microRNA-mediated gene regulation in animal cells. *Trends Genet.* **23**, 243–249. https://doi.org/10.1016/j.tig.2007.02.011.
14. Rani, V., Sengar, R.S., (2022). Biogenesis and mechanisms of microRNA-mediated gene regulation. *Biotechnol. Bioeng.* **119**, 685–692. https://doi.org/10.1002/bit.28029.
15. Sapkota, S., Pillman, K.A., Dredge, B.K., Liu, D., Bracken, J.M., Kachooei, S.A., Chereda, B., Gregory, P.A., Bracken, C.P., Goodall, G.J., (2023). On the rules of engagement for microRNAs targeting protein coding regions. *Nucleic Acids Res.* **51**, 9938–9951. https://doi.org/10.1093/nar/gkad645.
16. Ha, M., Kim, V.N., (2014). Regulation of microRNA biogenesis. *Nature Rev. Mol. Cell Biol.* **15**, https://doi.org/10.1038/nrm3838 8.
17. O'Brien, J., Hayder, H., Zayed, Y., Peng, C., (2018). Overview of microRNA biogenesis, mechanisms of actions, and circulation. *Front. Endocrinol.* **9**, 402. https://doi.org/10.3389/fendo.2018.00402.
18. Medley, J.C., Panzade, G., Zinovyeva, A.Y., (2021). microRNA strand selection: Unwinding the rules. *Wiley Interdisc. Rev. RNA* **12**, e1627.
19. Czech, B., Malone, C.D., Zhou, R., Stark, A., Schlingeheyde, C., Dus, M., Perrimon, N., Kellis, M., Wohlschlegel, J.A., Sachidanandam, R., Hannon, G.J., Brennecke, J., (2008). An endogenous small interfering RNA pathway in Drosophila. *Nature* **453**, 798–802. https://doi.org/10.1038/nature07007.
20. Ding, S.-W., Voinnet, O., (2007). Antiviral Immunity directed by small RNAs. *Cell* **130**, 413–426. https://doi.org/10.1016/j.cell.2007.07.039.
21. Pfeffer, S., Voinnet, O., (2006). Viruses, microRNAs and cancer. *Oncogene* **25**, https://doi.org/10.1038/sj.onc.1209915 46.
22. Hamilton, A.J., Baulcombe, D.C., (1999). A species of small antisense RNA in posttranscriptional gene silencing in plants. *Science* **286**, 950–952. https://doi.org/10.1126/science.286.5441.950.
23. Lindsay, M.A., (2008). MicroRNAs and the immune response. *Trends Immunol.* **29**, 343–351. https://doi.org/10.1016/j.it.2008.04.004.
24. Toledo-Arana, A., Repoila, F., Cossart, P., (2007). Small noncoding RNAs controlling pathogenesis. *Curr. Opin. Microbiol.* **10**, 182–188. https://doi.org/10.1016/j.mib.2007.03.004.
25. Wilkins, C., Dishongh, R., Moore, S.C., Whitt, M.A., Chow, M., Machaca, K., (2005). RNA interference is an antiviral defence mechanism in Caenorhabditis elegans. *Nature* **436**, https://doi.org/10.1038/nature03957 7053.
26. Frasca, F., Scordio, M., Scagnolari, C., (2022). Chapter 15—MicroRNAs and the immune system. In: Xiao, J. (Ed.), *MicroRNA*. Academic Press, pp. 279–305. https://doi.org/10.1016/B978-0-323-89774-7.00007-8.
27. Girardi, E., López, P., Pfeffer, S., (2018). On the importance of host microRNAs during viral infection. *Front. Genet.* **9** https://doi.org/10.3389/fgene.2018.00439.
28. Grassmann, R., Jeang, K., (2008). The roles of microRNAs in mammalian virus infection. *Biochimica et Biophysica Acta (BBA) – Gene Regulat. Mech.* **1779**, 706–711. https://doi.org/10.1016/j.bbagrm.2008.05.005.
29. Nahand, J.S., Mahjoubin-Tehran, M., Moghoofei, M., Pourhanifeh, M.H., Mirzaei, H.R., Asemi, Z., Khatami, A., Bokharaei-Salim, F., Mirzaei, H., Hamblin, M.R., (2020). Exosomal miRNAs: Novel players in viral infection. *Epigenomics* **12**, 353–370. https://doi.org/10.2217/epi-2019-0192.
30. Mukherjee, A., Di Bisceglie, A.M., Ray, R.B., (2015). Hepatitis C virus-mediated enhancement of microRNA miR-373 impairs the JAK/STAT signaling pathway. *J. Virol.* **89**, 3356–3365. https://doi.org/10.1128/JVI.03085-14.
31. Zhang, Y., Yang, L., Wang, H., Zhang, G., Sun, X., (2016). Respiratory syncytial virus non-structural protein 1 facilitates virus replication through miR-29a-mediated inhibition of interferon-α receptor. *Biochem. Biophys. Res. Commun.* **478**, 1436–1441. https://doi.org/10.1016/j.bbrc.2016.08.142.
32. Concepcion, C.P., Bonetti, C., Ventura, A., (2012). The miR-17-92 family of microRNA clusters in development and disease. *Cancer J (Sudbury, Mass.)* **18**, 262–267. https://doi.org/10.1097/PPO.0b013e318258b60a.
33. Zhu, Y., Huang, Y., Jung, J.U., Lu, C., Gao, S.-J., (2014). Viral miRNA targeting of bicistronic and polycistronic transcripts. *Curr. Opin. Virol.* **7**, 66–72. https://doi.org/10.1016/j.coviro.2014.04.004.
34. Tanzer, A., Stadler, P.F., (2004). Molecular evolution of a MicroRNA cluster. *J. Mol. Biol.* **339**, 327–335. https://doi.org/10.1016/j.jmb.2004.03.065.
35. Vilimova, M., Pfeffer, S., (2023). Post-transcriptional regulation of polycistronic microRNAs. *WIREs RNA* **14**, e1749.

36. de Pontual, L., Yao, E., Callier, P., Faivre, L., Drouin, V., Cariou, S., Van Haeringen, A., Geneviève, D., Goldenberg, A., Oufadem, M., Manouvrier, S., Munnich, A., Vidigal, J.A., Vekemans, M., Lyonnet, S., Henrion-Caude, A., Ventura, A., Amiel, J., (2011). Germline deletion of the miR-17∼92 cluster causes skeletal and growth defects in humans. *Nature Genet.* **43**, Article 10. https://doi.org/10.1038/ng.915.
37. Fang, L.-L., Wang, X.-H., Sun, B.-F., Zhang, X.-D., Zhu, X.-H., Yu, Z.-J., Luo, H., (2017). Expression, regulation and mechanism of action of the miR-17-92 cluster in tumor cells (Review). *Int. J. Mol. Med.* **40**, 1624–1630. https://doi.org/10.3892/ijmm.2017.3164.
38. Koralov, S.B., Muljo, S.A., Galler, G.R., Krek, A., Chakraborty, T., Kanellopoulou, C., Jensen, K., Cobb, B. S., Merkenschlager, M., Rajewsky, N., Rajewsky, K., (2008). Dicer ablation affects antibody diversity and cell survival in the B lymphocyte lineage. *Cell* **132**, 860–874. https://doi.org/10.1016/j.cell.2008.02.020.
39. Mestdagh, P., Boström, A.-K., Impens, F., Fredlund, E., Van Peer, G., De Antonellis, P., von Stedingk, K., Ghesquière, B., Schulte, S., Dews, M., Thomas-Tikhonenko, A., Schulte, J.H., Zollo, M., Schramm, A., Gevaert, K., Axelson, H., Speleman, F., Vandesompele, J., (2010). The miR-17-92 microRNA cluster regulates multiple components of the TGF-β pathway in neuroblastoma. *Mol. Cell* **40**, 762–773. https://doi.org/10.1016/j.molcel.2010.11.038.
40. Yang, H.-Y., Barbi, J., Wu, C.-Y., Zheng, Y., Vignali, P.D. A., Wu, X., Tao, J.-H., Park, B.V., Bandara, S., Novack, L., Ni, X., Yang, X., Chang, K.-Y., Wu, R.-C., Zhang, J., Yang, C.-W., Pardoll, D.M., Li, H., Pan, F., (2016). MicroRNA-17 modulates regulatory T cell function by targeting co-regulators of the Foxp3 transcription factor. *Immunity* **45**, 83–93. https://doi.org/10.1016/j.immuni.2016.06.022.
41. Zhao, W., Gupta, A., Krawczyk, J., Gupta, S., (2022). The miR-17-92 cluster: Yin and Yang in human cancers. *Cancer Treatment Res. Comm.* **33**, https://doi.org/10.1016/j.ctarc.2022.100647 100647.
42. Ota, A., Tagawa, H., Karnan, S., Tsuzuki, S., Karpas, A., Kira, S., Yoshida, Y., Seto, M., (2004). Identification and characterization of a novel gene, C13orf25, as a target for 13q31-q32 amplification in malignant lymphoma. *Cancer Res.* **64**, 3087–3095. https://doi.org/10.1158/0008-5472.CAN-03-3773.
43. He, L., Thomson, J.M., Hemann, M.T., Hernando-Monge, E., Mu, D., Goodson, S., Powers, S., Cordon-Cardo, C., Lowe, S.W., Hannon, G.J., Hammond, S.M., (2005). A microRNA polycistron as a potential human oncogene. *Nature* **435**, 828–833. https://doi.org/10.1038/nature03552.
44. Shi, B., Zhu, M., Liu, S., Zhang, M., (2013). Highly ordered architecture of microRNA cluster. *Biomed Res. Int.* **2013**, https://doi.org/10.1155/2013/463168 463168.
45. Khuu, C., Utheim, T.P., Sehic, A., (2016). The three paralogous microRNA clusters in development and disease, miR-17-92, miR-106a-363, and miR-106b-25. *Scientifica* **2016**, 1379643. https://doi.org/10.1155/2016/1379643.
46. Lewis, B.P., Burge, C.B., Bartel, D.P., (2005). Conserved seed pairing, often flanked by adenosines, indicates that thousands of human genes are microRNA targets. *Cell* **120**, 15–20. https://doi.org/10.1016/j.cell.2004.12.035.
47. Mogilyansky, E., Rigoutsos, I., (2013). The miR-17/92 cluster: A comprehensive update on its genomics, genetics, functions and increasingly important and numerous roles in health and disease. *Cell Death Differ.* **20**, Article 12. https://doi.org/10.1038/cdd.2013.125.
48. Rupaimoole, R., Slack, F.J., (2017). MicroRNA therapeutics: Towards a new era for the management of cancer and other diseases. *Nature Rev. Drug Discov.* **16**, https://doi.org/10.1038/nrd.2016.246 3.
49. Jung, Y.J., Kim, J.-W., Park, S.J., Min, B.Y., Jang, E.S., Kim, N.Y., Jeong, S.-H., Shin, C.M., Lee, S.H., Park, Y.S., Hwang, J.-H., Kim, N., Lee, D.H., (2013). C-Myc-mediated overexpression of miR-17-92 suppresses replication of hepatitis B virus in human hepatoma cells. *J. Med. Virol.* **85**, 969–978. https://doi.org/10.1002/jmv.23534.
50. Fu, Y., Zhang, L., Zhang, R., Xu, S., Wang, H., Jin, Y., Wu, Z., (2019). Enterovirus 71 suppresses miR-17-92 cluster through up-regulating methylation of the miRNA promoter. *Front. Micb.* **10** https://doi.org/10.3389/fmicb.2019.00625.
51. Choi, H.S., Jain, V., Krueger, B., Marshall, V., Kim, C.H., Shisler, J.L., Whitby, D., Renne, R., (2015). Kaposi's sarcoma-associated herpesvirus (KSHV) induces the oncogenic miR-17-92 cluster and down-regulates TGF-β signaling. *PLoS Pathog.* **11**, e1005255.
52. Triboulet, R., Mari, B., Lin, Y.-L., Chable-Bessia, C., Bennasser, Y., Lebrigand, K., Cardinaud, B., Maurin, T., Barbry, P., Baillat, V., Reynes, J., Corbeau, P., Jeang, K.-T., Benkirane, M., (2007). Suppression of MicroRNA-silencing pathway by HIV-1 during virus replication. *Science* **315**, 1579–1582.
53. Liu, Y.P., Haasnoot, J., ter Brake, O., Berkhout, B., Konstantinova, P., (2008). Inhibition of HIV-1 by multiple siRNAs expressed from a single microRNA polycistron. *Nucleic Acids Res.* **36**, 2811–2824. https://doi.org/10.1093/nar/gkn109.
54. Kincaid, R.P., Sullivan, C.S., (2012). Virus-encoded microRNAs: An overview and a look to the future. *PLoS Pathog.* **8**, e1003018.
55. Kincaid, R.P., Burke, J.M., Sullivan, C.S., (2012). RNA virus microRNA that mimics a B-cell oncomiR. *Proc. Natl. Acad. Sci.* **109**, 3077–3082. https://doi.org/10.1073/pnas.1116107109.
56. Bruscella, P., Bottini, S., Baudesson, C., Pawlotsky, J.M., Feray, C., Trabucchi, M., (2017). Viruses and miRNAs: More friends than foes. *Front Microbiol.* **8**, 824. https://doi.org/10.3389/fmicb.2017.00824.
57. Barbu, M.G., Condrat, C.E., Thompson, D.C., Bugnar, O. L., Cretoiu, D., Toader, O.D., Suciu, N., Voinea, S.C., (2020). MicroRNA involvement in signaling pathways during viral infection. *Front. Cell Dev. Biol.* **8**, 143. https://doi.org/10.3389/fcell.2020.00143.
58. Kincaid, R.P., Panicker, N.G., Lozano, M.M., Sullivan, C. S., Dudley, J.P., Mustafa, F., (2018). MMTV does not encode viral microRNAs but alters the levels of cancer-associated host microRNAs. *Virology* **513**, 180–187. https://doi.org/10.1016/j.virol.2017.09.030.
59. Baby, J., (2022). The Host miR-17-92 Cluster Negatively Regulates MMTV Replication by Targeting its Genomic

RNA via miR-92a Doctoral Thesis. United Arab Emirates (UAE) University.
60. Gull, B, Ahmad, W., Baby, J., Panicker, N. G., Khader, T. A., Rizvi, T. A., Mustafa, F. Identification and characterization of host miRNAs that target the mouse mammary tumor virus (MMTV) genome.
61. Mestdagh, P., Van Vlierberghe, P., De Weer, A., Muth, D., Westermann, F., Speleman, F., Vandesompele, J., (2009). A novel and universal method for microRNA RT-qPCR data normalization. *Genome Biol.* **10**, R64. https://doi.org/10.1186/gb-2009-10-6-r64.
62. Chugh, P., Dittmer, D.P., (2012). Potential pitfalls in microRNA profiling. *Wiley Interdisciplinary Rev. RNA* **3**, 601–616. https://doi.org/10.1002/wrna.1120).
63. Grunert, M., Appelt, S., Dunkel, I., et al., (2019). Altered microRNA and target gene expression related to Tetralogy of Fallot. *Sci. Rep.* **9**, 19063. https://doi.org/10.1038/s41598-019-55570-4.
64. Holt, M.P., Shevach, E.M., Punkosdy, G.A., (2013). Endogenous mouse mammary tumor viruses (Mtv): New roles for an old virus in cancer, infection, and immunity. *Front. Oncol.* **3**, 287. https://doi.org/10.3389/fonc.2013.00287.
65. Salmons, B., Knedlitschek, G., Kennedy, N., Groner, B., Ponta, H., (1986). The endogenous mouse mammary tumour virus locus Mtv-8 contains a defective envelope gene. *Virus Res.* **4**, 377–389. https://doi.org/10.1016/0168-1702(86)90084-5.
66. Mustafa, F., Al Amri, D., Al Ali, F., Al Sari, N., Al Suwaidi, S., Jayanth, P., Philips, P.S., Rizvi, T.A., (2012). Sequences within both the 5' UTR and Gag are required for optimal in vivo packaging and propagation of mouse mammary tumor virus (MMTV) genomic RNA. *PLoS One* **7**, e47088. https://doi.org/10.1371/journal.pone.0047088.
67. Aktar, S.J., Vivet-Boudou, V., Ali, L.M., Jabeen, A., Kalloush, R.M., Richer, D., Mustafa, F., Marquet, R., Rizvi, T.A., (2014). Structural basis of genomic RNA (gRNA) dimerization and packaging determinants of mouse mammary tumor virus (MMTV). *Retrovirology* **11**, 96. https://doi.org/10.1186/s12977-014-0096-6.
68. Chameettachal, A., Pillai, V.N., Ali, L.M., Pitchai, F.N.N., Ardah, M.T., Mustafa, F., Marquet, R., Rizvi, T.A., (2018). Biochemical and functional characterization of mouse mammary tumor virus full-length Pr77Gag expressed in prokaryotic and eukaryotic cells. *Viruses* **10**, 334. https://doi.org/10.3390/v10060334.
69. Mustafa, F., Vivet-Boudou, V., Jabeen, A., Ali, L.M., Kalloush, R.M., Marquet, R., et al., (2018). The bifurcated stem loop 4 (SL4) is crucial for efficient packaging of mouse mammary tumor virus (MMTV) genomic RNA. *RNA Biology.* **15**, 1047–1059.
70. Shackleford, G.M., Varmus, H.E., (1988). Construction of a clonable, infectious, and tumorigenic mouse mammary tumor virus provirus and a derivative genetic vector. *Proc. Natl. Acad. Sci. U.S.A.* **85**, 9655–9659.
71. Mallick, B., Ghosh, Z., Chakrabarti, J., (2009). MicroRNome analysis unravels the molecular basis of SARS infection in bronchoalveolar stem cells. *PLoS One* **4**, e7837.
72. Cao, H., Yu, W., Li, X., Wang, J., Gao, S., Holton, N.E., Eliason, S., Sharp, T., Amendt, B.A., (2016). A new plasmid-based microRNA inhibitor system that inhibits microRNA families in transgenic mice and cells: A potential new therapeutic reagent. *Gene Ther.* **23**, 527–542. https://doi.org/10.1038/gt.2016.22.
73. Grimson, A., Farh, K.-K.-H., Johnston, W.K., Garrett-Engele, P., Lim, L.P., Bartel, D.P., (2007). MicroRNA targeting specificity in mammals: determinants beyond seed pairing. *Mol. Cell* **27**, 91–105. https://doi.org/10.1016/j.molcel.2007.06.017.
74. Lewis, B.P., Shih, I.-H., Jones-Rhoades, M.W., Bartel, D. P., Burge, C.B., (2003). Prediction of mammalian microRNA targets. *Cell* **115**, 787–798. https://doi.org/10.1016/s0092-8674(03)01018-3.
75. Rehmsmeier, M., Steffen, P., Hochsmann, M., Giegerich, R., (2004). Fast and effective prediction of microRNA/target duplexes. *RNA (New York, N.Y.)* **10**, 1507–1517. https://doi.org/10.1261/rna.5248604.
76. Rennie, W., Kanoria, S., Liu, C., Mallick, B., Long, D., Wolenc, A., Carmack, C.S., Lu, J., Ding, Y., (2016). STarMirDB: A database of microRNA binding sites. *RNA Biol.* **13**, 554–560. https://doi.org/10.1080/15476286.2016.1182279.
77. Arvey, A., Larsson, E., Sander, C., Leslie, C.S., Marks, D. S., (2010). Target mRNA abundance dilutes microRNA and siRNA activity. *Mol. Syst. Biol.* **6**, 363. https://doi.org/10.1038/msb.2010.24.
78. Moi, L., Braaten, T., Al-Shibli, K., Lund, E., Busund, L.-T.-R., (2019). Differential expression of the miR-17-92 cluster and miR-17 family in breast cancer according to tumor type; results from the Norwegian Women and Cancer (NOWAC) study. *J. Transl. Med.* **17**, 334. https://doi.org/10.1186/s12967-019-2086-x.
79. Chaulk, S.G., Thede, G.L., Kent, O.A., Xu, Z., Gesner, E. M., Veldhoen, R.A., Khanna, S.K., Goping, I.S., MacMillan, A.M., Mendell, J.T., Young, H.S., Fahlman, R.P., Glover, J.N.M., (2011). Role of pri-miRNA tertiary structure in miR-17∼92 miRNA biogenesis. *RNA Biol.* **8**, 1105–1114. https://doi.org/10.4161/rna.8.6.17410.
80. Du, P., Wang, L., Sliz, P., Gregory, R.I., (2015). A biogenesis step upstream of microprocessor controls miR-17-92 expression. *Cell* **162**, 885–899. https://doi.org/10.1016/j.cell.2015.07.008.
81. Wang, S., Liu, P., Yang, P., Zheng, J., Zhao, D., (2017). Peripheral blood microRNAs expression is associated with infant respiratory syncytial virus infection. *Oncotarget* **8**, 96627–96635. https://doi.org/10.18632/oncotarget.19364.
82. Olive, V., Sabio, E., Bennett, M.J., De Jong, C.S., Biton, A., McGann, J.C., Greaney, S.K., Sodir, N.M., Zhou, A.Y., Balakrishnan, A., Foth, M., Luftig, M.A., Goga, A., Speed, T.P., Xuan, Z., Evan, G.I., Wan, Y., Minella, A.C., He, L., (2013). A component of the mir-17-92 polycistronic oncomir promotes oncogene-dependent apoptosis. *Elife* **2**, e00822.
83. Mu, P., Han, Y.-C., Betel, D., Yao, E., Squatrito, M., Ogrodowski, P., de Stanchina, E., D'Andrea, A., Sander, C., Ventura, A., (2009). Genetic dissection of the miR-17∼92 cluster of microRNAs in Myc-induced B-cell lymphomas. *Genes Dev.* **23**, 2806–2811. https://doi.org/10.1101/gad.1872909.
84. Olive, V., Li, Q., He, L., (2013). Mir-17-92, a polycistronic oncomir with pleiotropic functions. *Immunol. Rev.* **253**, 158–166. https://doi.org/10.1111/imr.12054.
85. Olive, V., Minella, A.C., He, L., (2015). Outside the coding genome, mammalian microRNAs confer structural and

functional complexity. *Sci. Signal.* **8**, re2. https://doi.org/10.1126/scisignal.2005813.
86. Stenvang, J., Petri, A., Lindow, M., Obad, S., Kauppinen, S., (2012). Inhibition of microRNA function by antimiR oligonucleotides. *Silence* **3**, 1. https://doi.org/10.1186/1758-907X-3-1.
87. Mayya, V.K., Duchaine, T.F., (2015). On the availability of microRNA-induced silencing complexes, saturation of microRNA-binding sites and stoichiometry. *Nucleic Acids Res.* **43**, 7556–7565. https://doi.org/10.1093/nar/gkv720.
88. Naeli, P., Winter, T., Hackett, A.P., Alboushi, L., Jafarnejad, S.M., (2023). The intricate balance between microRNA-induced mRNA decay and translational repression. *FEBS J.* **290**, 2508–2524. https://doi.org/10.1111/febs.16422.
89. Welte, T., Goulois, A., Stadler, M.B., Hess, D., Soneson, C., Neagu, A., Großhans, H., (2023). Convergence of multiple RNA-silencing pathways on GW182/TNRC6. *Mol. Cell* **83**, 2478–2492. https://doi.org/10.1016/j.molcel.2023.06.001.
90. Thomson, D.W., Bracken, C.P., Szubert, J.M., Goodall, G.J., (2013). On measuring miRNAs after transient transfection of mimics or antisense inhibitors. *PLoS One* **8**, e55214.
91. Brock, M., Trenkmann, M., Gay, R.E., Michel, B.A., Gay, S., Fischler, M., Ulrich, S., Speich, R., Huber, L.C., (2009). Interleukin-6 modulates the expression of the bone morphogenic protein receptor type II through a novel STAT3–microRNA cluster 17/92 pathway. *Circ. Res.* **104**, 1184–1191. https://doi.org/10.1161/CIRCRESAHA.109.197491.
92. O'Donnell, K.A., Wentzel, E.A., Zeller, K.I., Dang, C.V., Mendell, J.T., (2005). C-Myc-regulated microRNAs modulate E2F1 expression. *Nature* **435**, https://doi.org/10.1038/nature03677 7043.
93. Sylvestre, Y., De Guire, V., Querido, E., Mukhopadhyay, U.K., Bourdeau, V., Major, F., Ferbeyre, G., Chartrand, P., (2007). An E2F/miR-20a autoregulatory feedback loop. *J. Biol. Chem.* **282**, 2135–2143. https://doi.org/10.1074/jbc.M608939200.
94. Woods, K., Thomson, J.M., Hammond, S.M., (2007). Direct regulation of an oncogenic micro-RNA cluster by E2F transcription factors. *J. Biol. Chem.* **282**, 2130–2134. https://doi.org/10.1074/jbc.C600252200.
95. Ahmad, W., Panicker, N.G., Akhlaq, S., Gull, B., Baby, J., Khader, T.A., Rizvi, T.A., Mustafa, F., (2023). Global down-regulation of gene expression induced by mouse mammary tumor virus (MMTV) in normal mammary epithelial cells. *Viruses* **15**, 1110. https://doi.org/10.3390/v15051110.
96. Morley, K.L., Toohey, M.G., Peterson, D.O., (1987). Transcriptional repression of a hormone-responsive promoter. *Nucleic Acids Res.* **15**, 6973–6989. https://doi.org/10.1093/nar/15.17.6973.
97. Chen, C., Ridzon, D.A., Broomer, A.J., Zhou, Z., Lee, D. H., Nguyen, J.T., Barbisin, M., Xu, N.L., Mahuvakar, V.R., Andersen, M.R., Lao, K.Q., Livak, K.J., Guegler, K.J., (2005). Real-time quantification of microRNAs by stem-loop RT-PCR. *Nucleic Acids Res.* **33**, e179.
98. Chakraborty, S., Mehtab, S., Patwardhan, A., Krishnan, Y., (2012). Pri-miR-17-92a transcript folds into a tertiary structure and autoregulates its processing. *RNA* **18**, 1014–1028. https://doi.org/10.1261/rna.031039.111.
99. Wang, Z., Liu, M., Zhu, H., Zhang, W., He, S., Hu, C., Quan, L., Bai, J., Xu, N., (2010). Suppression of p21 by c-Myc through members of miR-17 family at the post-transcriptional level. *Int. J. Oncol.* **37**, 1315–1321.
100. Livak, K.J., Schmittgen, T.D., (2001). Analysis of relative gene expression data using real-time quantitative PCR and the $2-\Delta\Delta CT$ method. *Methods* **25**, 402–408. https://doi.org/10.1006/meth.2001.1262.
101. Kanoria, S., Rennie, W., Liu, C., Carmack, C.S., Lu, J., Ding, Y., (2016). STarMir Tools for Prediction of microRNA binding sites. *Methods Mol. Biol. (Clifton, N. J.)* **1490**, 73–82. https://doi.org/10.1007/978-1-4939-6433-8_6.
102. Rennie, W., Kanoria, S., Liu, C., Carmack, C.S., Lu, J., Ding, Y., (2019). Sfold tools for MicroRNA target prediction. *Methods Mol. Biol. (Clifton, N.J.)* **1970**, 31–42. https://doi.org/10.1007/978-1-4939-9207-2_3.
103. Olive, V., Bennett, M.J., Walker, J.C., Ma, C., Jiang, I., Cordon-Cardo, C., Li, Q.-J., Lowe, S.W., Hannon, G.J., He, L., (2009). MiR-19 is a key oncogenic component of mir-17-92. *Genes Dev.* **23**, 2839–2849. https://doi.org/10.1101/gad.1861409.